AD-A100 906 GENERAL ELECTRIC CO PHILADELPHIA PA SPACE DIV F/G 20/5
METAL VAPOR LASER CONTAMINANT STUDY.(U)
MAY 80 T W KARRAS, B G BRICKS F49620-79-C-0177
UNCLASSIFIED AFOSR-TR-81-0520 NL

1 OF 2
AD A
100906

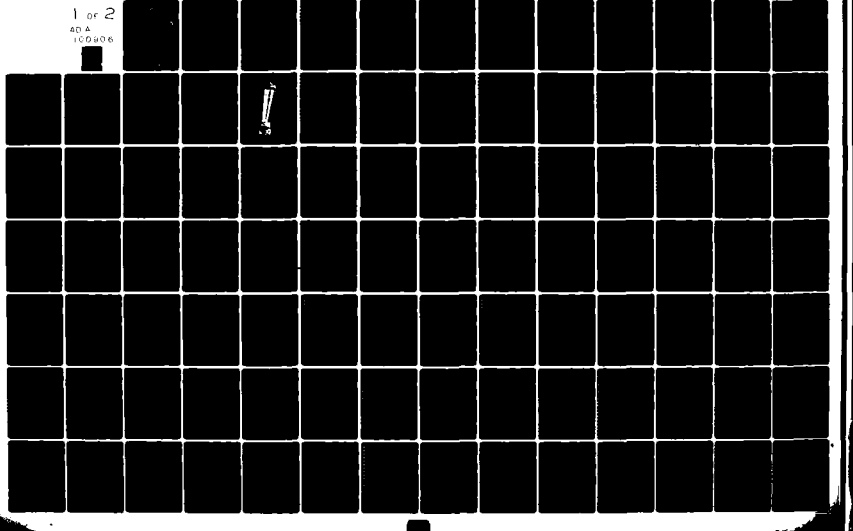

LEVEL II

METAL VAPOR LASER CONTAMINANT STUDY

FINAL REPORT

MAY 1980

PREPARED FOR

AIR FORCE OFFICE OF SCIENTIFIC RESEARCH

UNDER CONTRACT NO. F49620-79-C-0177

PREPARED BY

T. W. KARRAS
and
B. G. BRICKS

GENERAL ELECTRIC COMPANY
SPACE SYSTEMS DIVISION
P. O. BOX 8555
PHILADELPHIA, PA 19101

UNCLASSIFIED

SECURITY CLASSIFICATION OF THIS PAGE (When Data Entered)

REPORT DOCUMENTATION PAGE	READ INSTRUCTIONS BEFORE COMPLETING FORM
1. REPORT NUMBER (19) AFOSR-TR-81-0520	2. GOVT ACCESSION NO. AD-A100906	3. RECIPIENT'S CATALOG NUMBER
4. TITLE (and Subtitle) (6) METAL VAPOR LASER CONTAMINANT STUDY.	5. TYPE OF REPORT & PERIOD COVERED Scientific (9) Final rept.
	6. PERFORMING ORG. REPORT NUMBER
7. AUTHOR(s) (10) T. W. Karras, B. G. Bricks	8. CONTRACT OR GRANT NUMBER(s) (15) F49620-79-C-0177
9. PERFORMING ORGANIZATION NAME AND ADDRESS General Electric Company, Space Systems Div. P. O. Box 8555 Philadelphia, PA 19101	10. PROGRAM ELEMENT, PROJECT, TASK AREA & WORK UNIT NUMBERS (16) (17) 61102F 2301/A1
11. CONTROLLING OFFICE NAME AND ADDRESS AFOSR/NP Bolling AFB, Bldg. #410 Washington, DC 20332 (11)	12. REPORT DATE May 1980 (12) 203
	13. NUMBER OF PAGES v + 97
14. MONITORING AGENCY NAME & ADDRESS (if different from Controlling Office)	15. SECURITY CLASS. (of this report) Unclassified
	15a. DECLASSIFICATION DOWNGRADING SCHEDULE

16. DISTRIBUTION STATEMENT (of this Report)

Approved for public release; distribution unlimited.

17. DISTRIBUTION STATEMENT (of the abstract entered in Block 20, if different from Report)

18. SUPPLEMENTARY NOTES

19. KEY WORDS (Continue on reverse side if necessary and identify by block number)

Pulsed Metal Vapor Lasers
Copper Vapor Lasers
Lead Vapor Lasers
Contaminants
Wicks
Sealed-Off Lasers

20. ABSTRACT (Continue on reverse side if necessary and identify by block number)

Contaminants evolved during lead and copper vapor laser operation are identified. The principal long term source is the hot high density alumina discharge tube. Procedures for decontamination down to 10^{-6} mm partial pressure are described. Such decontamination is shown to be necessary for proper wick function and sealed-off operation. In conjunction with this work, a model has been demonstrated that relates metal vapor containment time to wick dimensions and a new sealed-off laser design has been successfully tested.

DD FORM 1 JAN 73 1473 EDITION OF 1 NOV 65 IS OBSOLETE

Unclassified 403025

SECURITY CLASSIFICATION OF THIS PAGE (When Data Entered)

ACKNOWLEDGMENTS

The work described in this report was supported by a combination of Air Force and GE 1979 IR&D funds. The work in Appendices 1 and 2 was largely G.E. supported and that in Appendix 3 was a mixture. In the body of the report most work done on the lead vapor laser was supported by Air Force funds and work on the copper laser by G.E. funds.

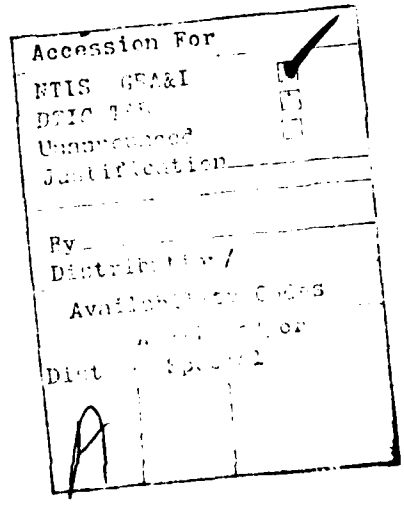

TABLE OF CONTENTS

LIST OF FIGURES

LIST OF FIGURES (Cont'd.)

LIST OF TABLES

LIST OF TABLES (Cont'd.)

I. INTRODUCTION

During the course of the General Electric metal vapor laser development program there have been several qualitative observations which are indicative of contaminating species in the buffer gas (helium)/metal vapor discharge mixture. For example, during break-in operation of a new ceramic discharge tube, the color of the discharge appears white rather than the typical pink color of the helium discharge. Furthermore, this condition is often accompanied by unstable discharge attachment at the cathode and arc formation. The latter causes current surges which often interfere with thyratron turn-off resulting in power supply trip-outs and long warm-up times.

Another indication of the presence of contaminating species is coating of the laser windows. This coating often builds up to such a degree that optical transmission is obscured. Laser operation is consequently seriously degraded.

These conditions generally improve markedly to acceptable levels in a matter of a few hours. However, laser performance often continues to show very gradual improvement over long periods of operation. These findings suggest a continual clean-up of contaminants released from the laser components. The slow flow of buffer gas, escaping through the unsealed ends of the laser tube to the highly evacuated region,[1,2] could carry such evolved species out.

This presence of contaminants is certainly not an unexpected finding. Laser tubes must be heated to 900-1000°C for the lead laser and to 1300-1400° for the copper laser. These values are substantially in excess of the normal vacuum bakeout temperature of 400°C needed to evolve trapped gases from the walls of high vacuum equipment. Clearly, these elevated temperatures should cause further species evolution. Furthermore, it is well known that even the

highest purity alumina tubes have significant percentage concentrations of various metal oxides which could be evolved during operation.

These contaminants did not seem, during the early years of development, to have seriously hindered the dramatic steps forward in laser performance. In fact it seems to be a generally accepted tenant that these high gain lasers would not only operate but perform well under dirty conditions which would prevent other types of lasers from even reaching threshold.

Now, however, the progress in metal vapor laser development has come to a point where further improvements in power and efficiency and especially long-life, sealed-off operation will require a better understanding of the role contaminants play and how to minimize their deleterious effects. This need has become quite evident in our laboratory where recirculating wick structures are used for metal vapor containment during long term operation. It has been learned that the wetting properties, and hence ultimately operating lifetime, of the liquid metal on the wick surface are very sensitive to contaminants and surface preparation.

Also, there have been recent reports from other laboratories on work and observations concerning the problem of contamination. Smilanski et al[3] have noted a correlation between the decay of the sodium line intensity (and presumably a correspondingly smaller sodium concentration) in a copper laser and an increase in laser performance. They also note that lasing in a high pressure neon buffer, which also enhances laser performance in their apparatus, seemed to correlate with the use of high purity alumina discharge tubes and long term processing.

In our laboratory prior to this study we had begun to make preliminary

spectroscopic measurements to positively identify contaminating species in the laser discharge. The purpose of this study is to pursue further this spectroscopic identification of the contaminating species and to determine their time evolution under various experimental conditions. As a direct result of this activity we expected to develop a physical picture and appropriate procedures to ensure that the levels of contamination are reduced to acceptable levels prior to long-term laser operation.

II. TEST FACILITIES

Three facilities were assembled and dedicated to the experimental testing performed during the course of this program. In this section each facility is described in detail, and a brief explanation of the type of tests performed at each is presented.

Facility 1: In this facility ceramic laser discharge tubes were heated by the discharge-heated technique to temperatures several hundred degrees centigrade above normal operating temperatures for a lead laser and maintained at this condition for extended periods of time. The purposes were: 1) to identify and monitor spectral line intensities of contaminating species during such bakeout procedures, and 2) prepare tubes for laser tests in other facilities to evaluate the bakeout process. This facility is shown schematically in Figure 1 and consisted of the following components:

i) Laser Vacuum Jacket: assembled from standard stainless steel Varian vacuum components with copper gasket seals, a vacuum break, and two water-cooled window assemblies with demountable windows,[1,2]

ii) Diffusion/Forepump pumping station with appropriate pressure monitoring devices,

iii) Gas handling system to admit buffer gas(es) to the laser tube,

iv) Pulse Discharge Electronics: capacitor pulse forming network, hydrogen thyratron, resonant charge circuit, trigger pulse generator, high voltage power supply,

v) Diagnostic Equipment: monochromator with photomultiplier, current and

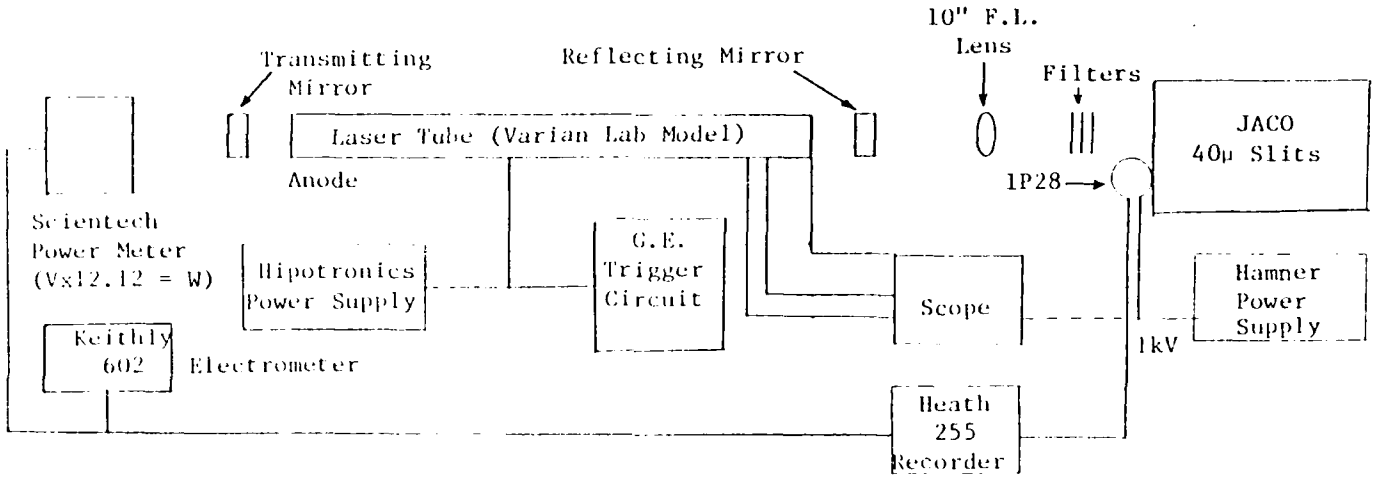

FIGURE 1. BAKEOUT FACILITY SCHEMATIC

voltage probes, oscilloscopes, chart recorders, electrometer.

Facility 2: This facility was used to perform extended laser life tests. The purpose was to evaluate the effects of bakeout and contaminant reduction on the long life performance of the lead laser wicks. The experimental set-up is shown schematically in Figure 2 and consisted of the following:

i) Laser Vacuum Jacket: assembled from standard stainless steel Varian vacuum components with copper gasket seals, a vacuum break, and two water-cooled window assemblies with demountable windows,[1,2]

ii) Diffusion/Forepump pumping station with appropriate pressure monitoring devices,

iii) Gas handling system to admit buffer gas(es) to the laser tube,

iv) Pulse Discharge Electronics: capacitor pulse forming network, hydrogen thyratron, resonant charge circuit, trigger pulse generator, high voltage power supply,

v) Diagnostic Equipment: monochromator, laser power meter, recorder, electrometer.

Facility 3: This facility was specially constructed from components having all metal seals (no O-rings) in order to have a system capable of being sealed-off to evaluate the degree of, and effects due to, contamination build-up during the course of long-term sealed-off operation. As described below and shown in Figure 3, the system was designed for sealed-off operation without the laser tube being sealed-off from the vacuum jacket region.

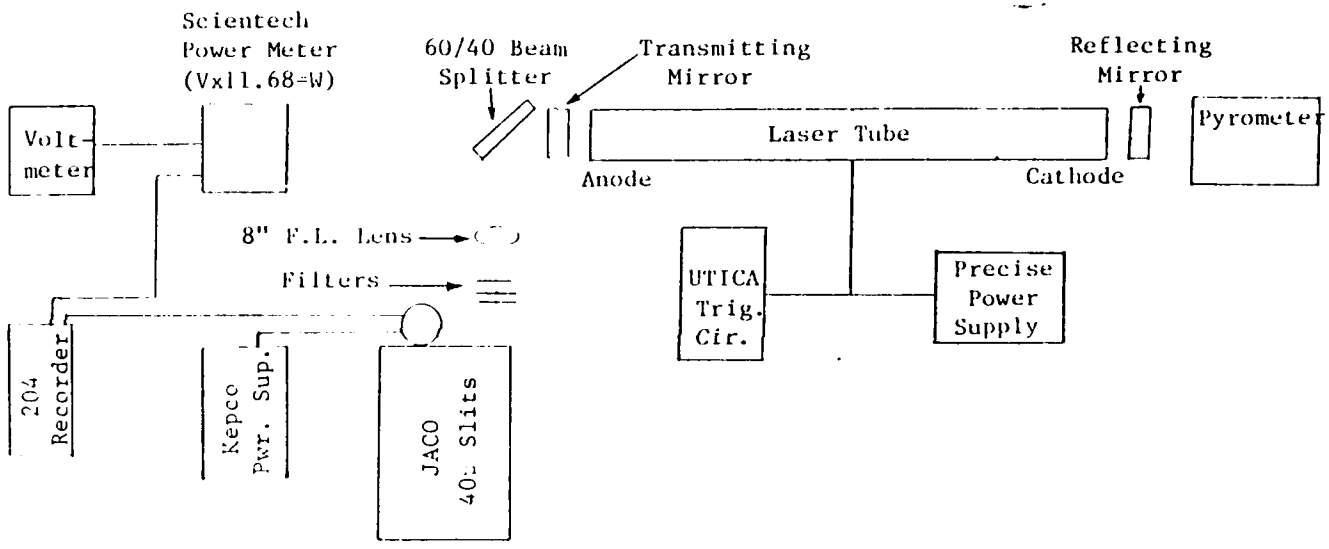

FIGURE 2. LIFE TEST FACILITY SCHEMATIC

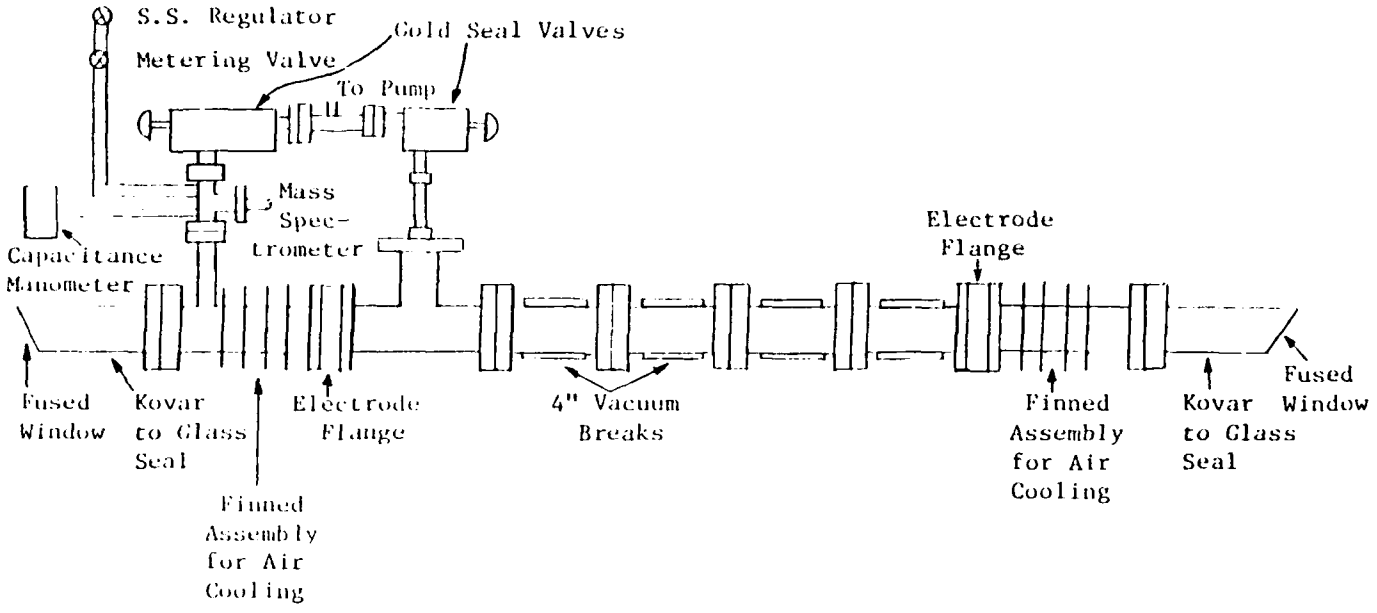

FIGURE 3. SEALED OFF LASER FACILITY

i) Laser vacuum jacket was assembled principally from a series of vacuum breaks. The laser tube was supported between electrode flanges and surrounded with zirconia and Saffil to provide thermal insulation and to prevent electrical breakdown. This was necessary because the tube was not sealed, and hence the buffer gas pressure in and outside of the tube are equal. Finned sections were provided to thermally isolate the fused glass window assemblies (see Appendix I).

ii) Diffusion/Forepump pumping station with appropriate pressure monitoring devices; gold seal valves were used to connect tube and jacket regions to the pump line; all stainless regulator was used to admit high purity buffer gas. A capacitance manometer was installed to measure pressure during sealed-off operation.

iii) Gas handling system to admit buffer gas(es) to the laser tube.

iv) Pulse Discharge Electronics: capacitor pulse forming network, hydrogen thyratron, resonant charge circuit, trigger pulse generator, high voltage power supply.

v) Diagnostic Equipment: monochromator, voltage probe, oscilloscope, laser power meter, recorder, electrometer, mass spectrometer.

Several facilities similar to those shown in Figures 1 and 2 were also used for short term testing. A standard General Electric Model 6-15 copper vapor laser (Figure 4) was used for many of these.

The laser tubes used for the lead vapor laser tests were all 1 1/4" alumina ID 24" long. Thermal shielding of 2-3 layers of tantalum foil was used, depending upon the temperature sought. The copper vapor laser tubes tested were

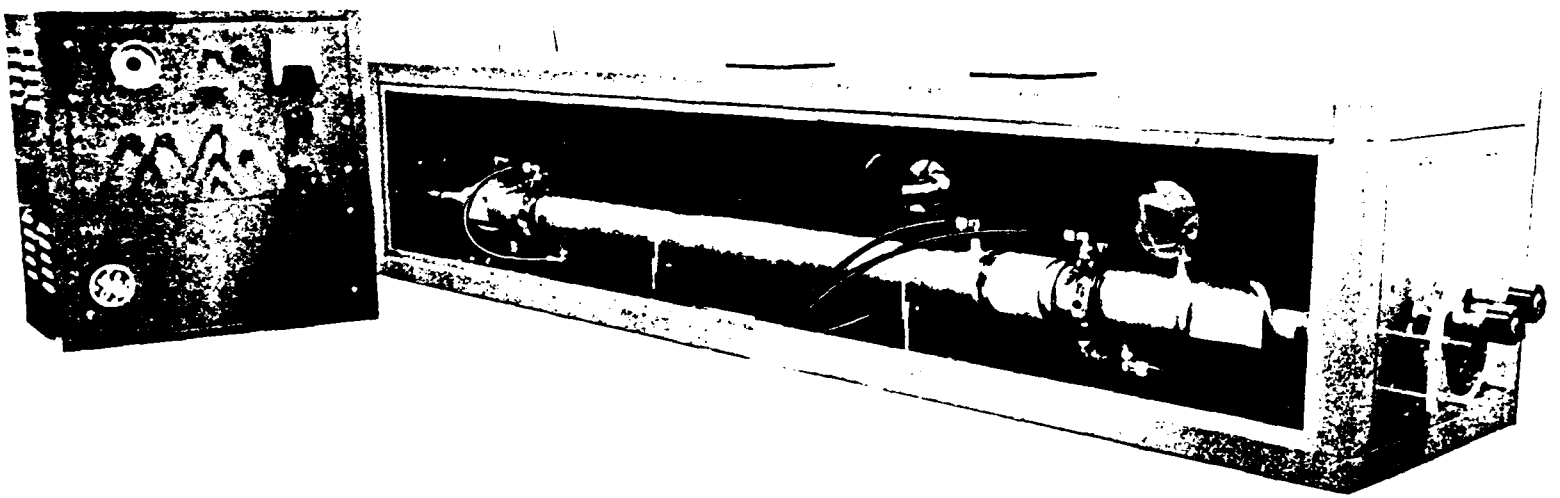

generally those of standard Model 6-15 design, 1" ID 42" long. Thermal shields were made of 10-13 layers of molybdenum foil. A few tests were also conducted with 1 1/4" ID copper vapor laser tubes.

III. CHARACTERISTICS OF OPERATION

A. General

The general characteristics of operation of the lasers investigated are summarized in References 2,4-6. Both lead and copper vapor lasers were involved. The relevant structure of both is schematically shown in Figure 5.

During operation the region inside the ceramic discharge tube, electrodes, and window assemblies is filled with an inert gas and discharge. The most intense discharge takes place between the electrodes since the primary discharge attachment occurs on these components. However, visible current attachment can be seen well into the window assembly, at times extending up to the windows. Similarly, the highest temperature regions of the device are inside the ceramic tube and to a lesser degree out to the wicks and electrodes. The surrounding thermal radiation shields for this study were designed for maximum ceramic tube temperatures of over 1500°C in a copper vapor laser and 1300°C in a lead vapor laser. Operating temperatures are respectively 1400°C and 1000°C. The window assemblies are water or air cooled and so their temperature is close to that of the ambient environment.

In all but the sealed tube design, there is a continuous slow leak of buffer gas through the slip joints between the electrodes and the ceramic and between the electrodes and the flanges through which they are inserted. This flow of gas prevents any contaminants evolved in the evacuated space surrounding the discharge tube from entering the region filled with discharge. Non-condensible contaminants evolved within the gas filled region will, of course, be carried out with the flow.

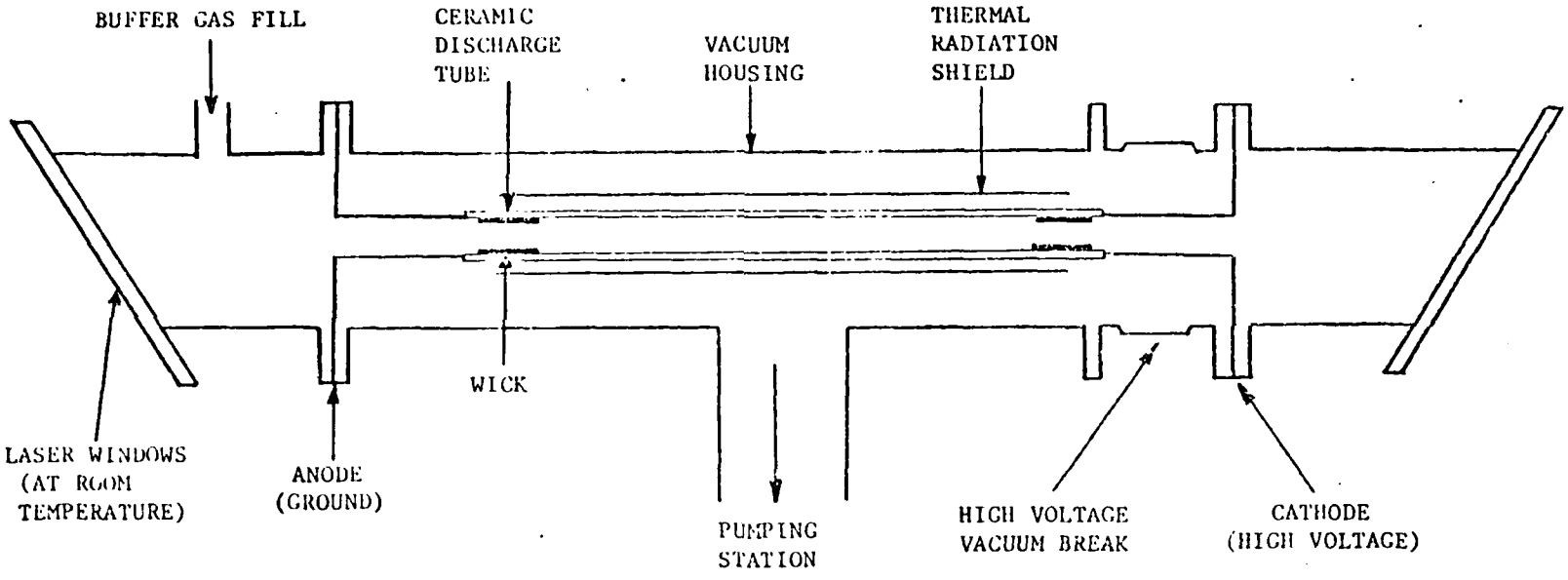

FIGURE 5. SCHEMATIC DIAGRAM OF DISCHARGE-HEATED METAL VAPOR LASER

Ideally the only species to be found in the gas phase would be the inert gas (helium in these experiments) and the metal vapor of choice (copper or lead). Small amounts of hydrocarbons (pump oil) and atmospheric constituents were expected to be driven off relatively easily. Thereafter "clean" conditions might be expected.

This ideal model was only partly borne out by observations. Initial discharge appearance was the blue-white characteristic of atmospheric constituents adsorbed on various surfaces. During this time hydrocarbons were also driven off and, in part, deposited on the laser windows. The current drawn from the high voltage supply during this period was found to be anomalously high for the voltage applied. If heated sufficiently to vaporize copper or lead only poor laser output could be obtained.

During a period of a few minutes to several hours, depending upon whether the tube had been run previously, the color of the discharge gradually became the pink characteristic of a helium discharge. The hydrocarbon coating of the window slowed and the current fell. The laser power gradually improved.

The appearance of steady state was then reached in which the discharge was pink to the eye and coating of the window was slow. The power supply current held steady. The only gross evidence that a true steady state had not been reached was the continuing improvement in laser output power. This stage continued for many hours.

B. Impurities

Upon closer examination the presence of a host of potential impurities can be deduced. Table 1 lists the impurities shown by vendor analysis to be present in the materials used in hot sections of the laser. The high vapor pressure of

TABLE 1

IMPURITY CONTENT

	Alumina* (Discharge Tube)	Tantalum (Electrodes & Wick)	Tungsten (Wick)	304 Stainless Steel (Flanges Window Assembly)
Fe	M	M	C	P
Ni		M	C	P
Si	M	M	C	P
Al	P		C	
B	C			
Ca	M		C	
Cr	X		C	P
Cu	X	C	C	
Ga	M			
Pb			C	
Mg	M		C	
Mn	C		C	P
Na	M			
Nb		M		
P				M
S				M
Sn			C	
Ti	C	M	C	
C		M	C	M
O	P	M		
H		C		
N		M		
W		M	P	
Mo		M		
Hf	M			
Ta		P		

*In the form of oxides.

P = Primary Constituent
M = Major contaminant 01~.01%
C = Minor contaminant .01~.001%
X = Trace

some of these species would be expected to drive them into the discharge vapor during high temperature operation. In addition, the atmosphere used to sinter the tubes includes atmospheric gases, natural gas, and obvious products such as water, CO, and CO_2. These gases would be trapped in the grain boundaries and closing pores of the alumina.[12]

In addition to gaseous impurities such as oxygen, nitrogen, and hydrogen the highest vapor pressure materials among these contaminants are listed in Table 2. The most easily vaporized (phosphorous and sulfur) are only found in the well-cooled window assembly and so may never appear. The others are in the discharge tube, the highest temperature point, and so are to be expected. However, the impurities there are in the form of oxides with generally low vapor pressure.

High temperatures are not the only environment parameter that can introduce impurity species to the discharge plasma. Sputtering and other discharge-surface interaction mechanisms can be very effective in this role. In addition, heavy metals like tungsten, tantalum, and iron can be released into the discharge plasma by this mechanism. They are abundant in the metals making up the laser.

It is the ultimate clean up of the impurities evolved by these two processes during the last stage of operation that will be the principal subject of this report.

C. Current-Voltage Characteristics

As mentioned earlier, during the early stage of laser tube heat up molecular contaminants are driven off. This changes the discharge color and reduces the high voltage power supply current. During this period the current is susceptible to large transients that can momentarily overload the power supply,

TABLE 2

VAPOR PRESSURE OF SOLID IMPURITIES
1700°K

METAL	VAPOR PRESSURE
S, P, Na, Mg, Ca, Mn, Pb	>10 torr
Al	5×10^{-1}
Cu	10^{-1}
Cr	5×10^{-2}
Ni, Fe, Ga	5×10^{-3}
Si	5×10^{-4}
Ti	10^{-4}

tripping out its protective interlock. For a fixed supply voltage the current will gradually fall to a value as much as 25% below its maximum. Thereafter, when the laser is exposed to air the current will run at an intermediate level for a short time before returning to its "clean" value. Table 3 summarizes these observations for a low power inadequate to heat the discharge tube but enough to vaporize laser metal.

For higher input power, sufficient to heat the discharge tube to a temperature that will vaporize laser metal, the reverse process occurs. The power supply current rises. The same power will produce a constant or falling current if the metal vapor pressure is low. Table 4 shows how the current rises as the metal vapor pressure rises for a copper vapor laser. The laser output power is included as a measure of that vapor density. It is interesting to note that the fall in current and rise in laser power between the last two readings may reflect continuing clean up of discharge impurities.

TABLE 3

BEHAVIOR OF POWER SUPPLY CURRENT
AS LASER CLEANS UP

CURRENT	DISCHARGE APPEARANCE	CONDITION
250 ma	Blue	Unheated
250 ma	Pink but dim	Previously moderately heated.
230 ma	Pink & bright	Previously well heated or after long term laser operation and short air exposure.
200 ma	Pink & bright	After long term laser operation, no air exposure.

Power supply voltage, 3.0 Kv, 5 torr helium buffer. Laser loaded with copper or lead. Results are the same since tube is cold.

TABLE 4

BEHAVIOR OF POWER SUPPLY CURRENT
AS COPPER VAPOR PRESSURE IN
DISCHARGE IS INCREASED

ELAPSED TIME	CURRENT	COPPER LASER POWER
0	300 ma	-
0:20	340 ma	1.22 watts
0:36	365 ma	6.89 watts
1:35	372 ma	9.47 watts
4:32	370 ma	10.63 watts

Copper Vapor Laser: 4.8 torr Helium Buffer
5.5 Kv power supply voltage

IV. WINDOW COATING

As described in the previous section, laser windows were found to be coated by discharge impurities in two stages. The first stage involved hydrocarbons and lasted only a short period. The coating was often so opaque that laser operation was impaired. It should be noted that even with clean windows laser operation was at best poor during this early stage, but with coated windows the power remained low. Consequently, the windows were then usually removed and wiped off or polished. This coat was rarely strongly adhering.

The second stage involved a more slowly growing window coating composed primarily of sputtered products of window assembly (304 stainless steel) materials. Appendix 2 describes the characteristics of this coating and a means for preventing its growth. As described in that appendix, sputter coating of the window can be minimized by placing a non-conducting shield next to the window. This forces current attachment to be remote and sputter products cannot reach the window.

Another window coating mechanism that continues even when sputter coating is suppressed involves diffusion of droplets of the lasing metal. Inadequate confinement of the laser metals to the hot zone of the discharge tube allows some to condense on the windows, often limiting laser output before loss of metal from the hot zone has the same effect.

Two techniques have been used to produce that confinement. The most common uses high buffer pressures to restrict diffusion and so is operative in most metal vapor lasers to at least some degree. The use of 200-300 torr of neon can keep windows clean for over 3,000 hours.[7] Unfortunately the use of this technique leads to a decrease in power output of 25-30%.

Another technique in common use involves wick structures to recirculate metal diffusing out of the hot zone of the laser.[8,9] With proper design wick structures can be made that prevent laser metal from reaching (coating) windows for very long periods. Appendix 3 and a section to follow describe how impurities in the plasma affect such operation.

V. IDENTIFICATION OF SPECIES

Spectroscopic analysis of the discharge provides some insight into the causes for continuing improvement in laser output. Several contaminant lines of decreasing intensity can be identified. The effects of some of these species have already been correlated with reduced laser power.[10]

As might be expected the species and line intensities observable are dependent upon laser tube history, operating temperature, discharge power, and presence of laser metal. The conditions that bring out many of the strongest impurity lines are:

1) A fresh unheated discharge tube,
2) Run at maximum temperature,
3) With maximum input power,
4) Without any laser metal.

The initial clean-up (to be discussed later) of a copper laser tube before introduction of copper is typical of such operation.

The impurities producing the strongest spectral lines under these conditions and the lines generally used for identifying them are listed in Table 5. It should be noted that the majority are represented by ionic as well as neutral species.

In contrast to these results operation at lower power in a cold tube produced stronger lines from all the same gases (nitrogen, oxygen, and hydrogen), but very few of the metal species. Only the strongest lines of calcium, lead, and sodium appeared, and those weakly. In addition, two oxides (lead and calcium) were identified. Table 6 lists all the lines found under

TABLE 5

IMPURITY SPECTRAL LINES*
IN ANGSTROMS

Ca	3933.67	4226.73	4425.44	4434.96	4454.78
	6162.17				
Ca^+	3158.87	3179.33	3933.66	3968.47	
Cr	3578.69	3605.33	4254.3	4274.8	4289.7
	5206.04	5208.44			
Cr^+	2835.63	2843.25	2849.83		
Cu	3247.54	3273.96	5105.54	5218.2	5782.13
Fe	3570.1	3719.94	3734.87	3737.13	3749.49
	3758.24	3285.88	3859.91		
Fe^+	2598.37				
Ga	2874.24	2943.64	4172.06		
H	4340.47	4631.88	4634	4861.33	4928.7
	5812.58				
He	3613.64	3888.65	4026.19	4387.9	4471.5
	4713.2	4921.9	5015.7	5047.7	5875.9
Li	2741.2	3232.61	4602.86	4971.99	6103.64
Mg	2852.13	3829.35	3832.31	3838.26	5167.34
	5172.7	5183.51	5528.46		
Mg^+	2795.53	2802.69			
Mn	4030.76	4033.07	4034.49	4041.36	
Mn^+	2576.10	2593.73	2605.69		
N	3830.39	4099.94	4109.98	4151.46	4935.83
	6008.48	5200.5			
N^+	5005.14	5679.56			
N_2	3576.9	3755.4	3804.9		

*Conditions: 1400°C, 2000 watts input, helium buffer, no laser metal except very small fragments; possibly on electrodes.

TABLE 5 (Cont'd.)

N_2^+	3582.1	3884.3	3914.4	4278.1	4336.5
Na	3302.32	3302.99	5682.66	5688.22	5889.95
	5895.92				
Ni	3414.76	3492.96	3515.05	3524.54	
O	3823.47	3947.33	4368.3	5330.66	6158.2
O_2	3517				
Ti	3642.88	3653.50	3998.64	4981.73	
Ti^+	3349.41	3361.21	3361.64		

TABLE 6

LINES OBSERVED IN COLD LASER TUBE*

He	3888.7	4471.5	4921.9	4713.7	4387.9
	5015.7	5047.7	3964.7	3613.64	4025.19
	5875.9	4437			
H	4861.3	4340.5			
O	4368.3	5330.7			
O_2	3914	3743	3671		
O_2^+	3859.5				
N_2	4278.1	3914.4	3576.9	5030.8	3804.9
	3940.3	4141.8	3536.7	3755.4	4710.5
	4200.5				
N_2^+	4278	3582	4599.7	4651.8	4709.2
	4236.5	3884.3			
Ca^+	3968.47				
Na	5689.95	5995.92			
Pb	4057.83				
PbO	4553.7				
CaO	3564				

*Conditions: <550°C, 590 watts input, helium buffer, no laser metal except for very small fragments possibly still on electrodes.

this condition.

It is important to note here the absence and presence of various species in the discharge plasma. Tungsten, tantalum, aluminum, and silicon, among the most important constituents of the laser tube assembly, cannot be clearly identified. On the other hand, some trace species such as titanium, manganese and calcium are represented by very strong spectral lines. These trace species as well as all the dominant spectral impurities are present within the high density alumina discharge tube and have high vapor pressure. This component of the laser must consequently be the source of the impurities and must release them only upon sufficient heating. Low vapor pressure substances (W and Ta) and those bound strongly (Al and Si) will not be evolved.

This model will be supported in succeeding sections.

VI. EVOLUTION OF CONTAMINANTS WITH TIME

A. General

The contaminants discussed in the previous section were generally found to decrease with time as the discharge was operated. Increase in input power and tube temperature would temporarily increase contaminant line intensity, but only to fall again. The obvious conclusion to be drawn is that the various contaminant species were being depleted from some reservoir internal to the discharge tube.

The mechanism of this depletion could be thermal in character or could involve some discharge related process. Long term experiments at different temperatures and with both furnace and discharge heating were conducted to allow differentiation between the two mechanisms.

B. Laser Operation

Typically a metal vapor laser in our laboratory has been heated gradually to its working temperature over a period of one to two hours. Heat-up periods of less than 1/2 hour have also been used but that requires discharge operation at maximum input power from the start. Since most of our experiments have involved laser tubes that have been recently exposed to the atmosphere and some period of "clean-up" has generally been required, such short heat-up periods have been rare. Tests and practical applications that allow continued use of a laser without exposure to the atmosphere are another question, of course.

The intensities of most spectral lines are found to increase continuously during typical laser heat-up (Table 7). The most volatile elements, nitrogen, hydrogen, and sodium have spectral lines that show signs of decrease, even

TABLE 7

RELATIVE INTENSITIES OF SPECTRAL LINES
DURING TYPICAL COPPER LASER WARM-UP

		Cold Tube Blue Discharge 945 W In	Hot Tube Pink Discharge 1577 W In 1 W Out	Very Hot Tube 1950 W In 12 W Out	Very Hot Tube After 98 Hours Run 2266 W In 13 W Out
He	5873	2×10^{-5}	1.4×10^{-4}	1.5×10^{-4}	1.9×10^{-4}
H	4340	4.5×10^{-7}	5.4×10^{-6}		7.5×10^{-6}
Cu	5782	*	6×10^{-5}	2.7×10^{-4}	3.1×10^{-4}
Na	5889	*	4.3×10^{-6}	6.3×10^{-6}	2.25×10^{-6}
	5895	*	2.5×10^{-6}	3.7×10^{-6}	1.85×10^{-6}
Ca	4455	*	3.7×10^{-7}		2.4×10^{-6}
Fe	4271		5×10^{-7}		2.5×10^{-6}
N	4100	2.5×10^{-7}	1.5×10^{-6}	1.9×10^{-6}	1.8×10^{-6}

*Very small

before the time full operating power is reached. At this time the contaminant line intensities are all about two orders of magnitude below those of copper and helium.

The time development of contaminant species can be seen more clearly by following line intensities through a long heat-up cycle followed by an even longer period of steady heating. This has been done with a fresh lead vapor laser discharge tube brought up to maximum for the first time in 16 hours and then heated for another 64 hours. Figures 6 and 7 show how several of the most important spectral intensities varied. As might be expected helium line intensities (Figure 6) approach maximum with the input power and during long term constant inupt power operation remain roughly constant. The same figure shows that hydrogen and oxygen line intensities peak after only 7 hours well before maximum input power has been reached. This is consistent with the depletion of a source of both gases (e.g., hydrocarbons) at this time. Thereafter, the lines of both, as those of all the other discharge species, decrease roughly exponentially. Table 8 lists the values of the e^{-1} time.

The only other gas, nitrogen (Figure 7), has a later line intensity peak and a much larger ultimate clean-up rate (Table 8). Clearly the source of nitrogen is quite different from that of hydrogen and oxygen.

Sodium and lead line intensities peak with the nitrogen lines and the input power. All three have long term clean-up rates related inversely to the square root of the atomic (or molecular) mass, as is the short term rate for oxygen (Table 8). Such a relationship is indicative of loss limited by diffusion through the helium buffer.

Calcium, the only other metal contaminant with lines of measurable intensity

FIGURE 6. VARIATION OF SPECTRAL LINE INTENSITIES DURING LONG TERM OPERATION OF A LEAD VAPOR LASER. HELIUM, HYDROGEN, AND OXYGEN. INPUT POWER AND DISCHARGE TUBE TEMPERATURE ARE INCLUDED FOR REFERENCE. LONG TERM TUBE TEMPERATURE 1150°C.

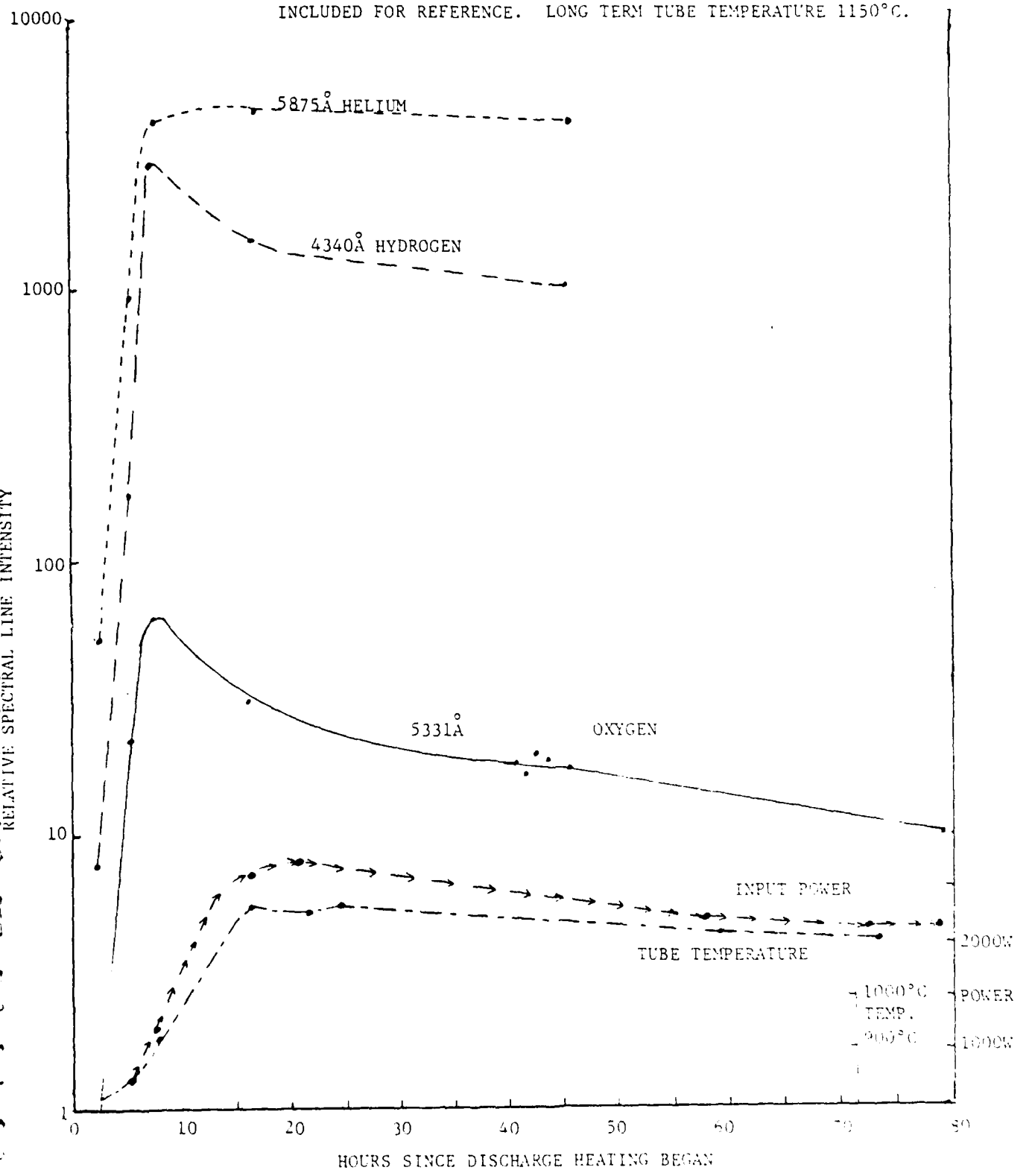

FIGURE 7. VARIATION OF SPECTRAL LINE INTENSITIES DURING LONG TERM OPERATION OF A LEAD VAPOR LASER. CALCIUM, LEAD, NITROGEN AND SODIUM.

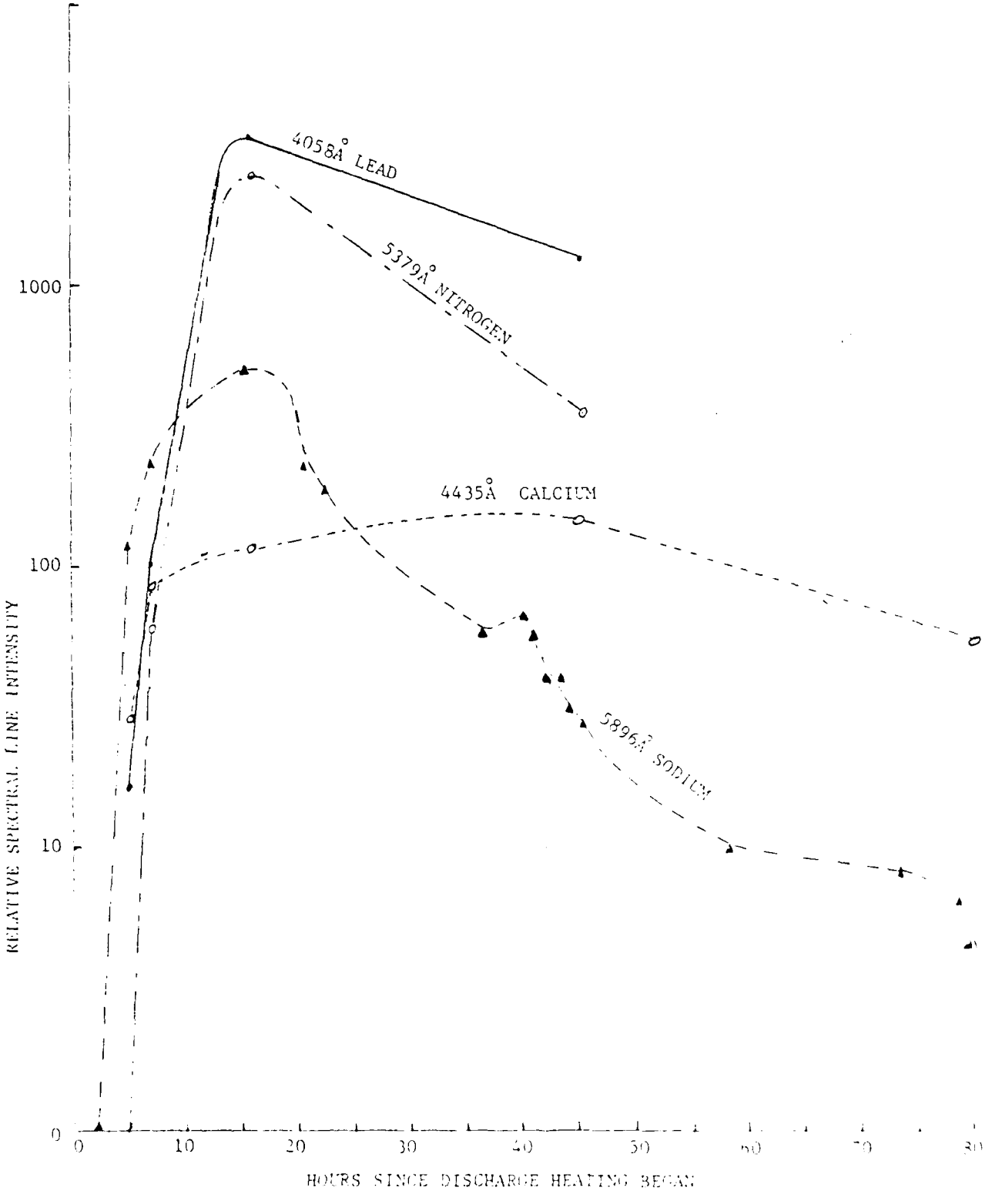

TABLE 8

LONG TERM CLEAN-UP RATE FOR
VARIOUS CONTAMINANTS

	e^{-1} Time From Data on Figs. 6 & 7[+]		Diffusion Controlled e^{-1} Time Scaled to that of Lead*
	Short Time	Long Time	α'
Hydrogen	.090 hr^{-1}	.012 hr^{-1}	.33 hr^{-1}
Oxygen	.090	.019	.084
Lead		.033	-
Calcium		.029	.075
Nitrogen		.086	.089
Sodium		.088	.088

*$\alpha' = \left(\frac{M_{pb}}{M_x}\right)^{1/2} .033$

[+]Averaged with values determined from other spectral lines of the same species.

appearing at these temperatures (Figure 7), peaks at an even later time . Furthermore, like the long term rate of hydrogen and oxygen, its decay rate is well below what might be expected from diffusion.

Once the laser tube is cooled and then reheated, line intensities initially rise to higher levels than they had just before the discharge was extinguished and then decay exponentially as before. Figure 8 shows the development of sodium line (5876A) intensity during such a reheating and the decay rate during the first run preceeding it for comparison. It should be noted that the line intensity peak is well below that of the first run and the decay rate immediately following is similar to that of the first run. However, a secondary maximum appears obscuring the long term decay. Such secondary maxima can also be seen in the latter part of run 1 on this figure and on Figure 7.

Exploration of higher temperature ranges has been made with a copper laser tube (Figures 9 and 10). The principal difference from the lead laser experiments just discussed lies in the added thermal radiation shielding, allowing 2000 watt input power to produce discharge tube temperature of over $1400^{o}C$ - $1500^{o}C$, and the fact that this was not a new tube. Figure 8 shows initial heat-up and Figure 9 shows two runs that followed.

The general pattern of an initial peak in line intensity followed by an exponential decay is repeated. Decrease in peak amplitude with each succeeding reheat is also repeated. The gradual increase in input power shown on Figure 9 produces a long term decline in sodium line intensity after that first peak, until a time-temperature condition produces a second peak. Successive reheating produced only the expected primary peak and a decay rate of the sodium line (Figure 10) of $.09hr^{-1}$, the same as was found for the lead laser in Figure 7 and

FIGURE 8. SODIUM LINE (5896Å) INTENSITY DEVELOPMENT DURING DISCHARGE TUBE REHEATING.

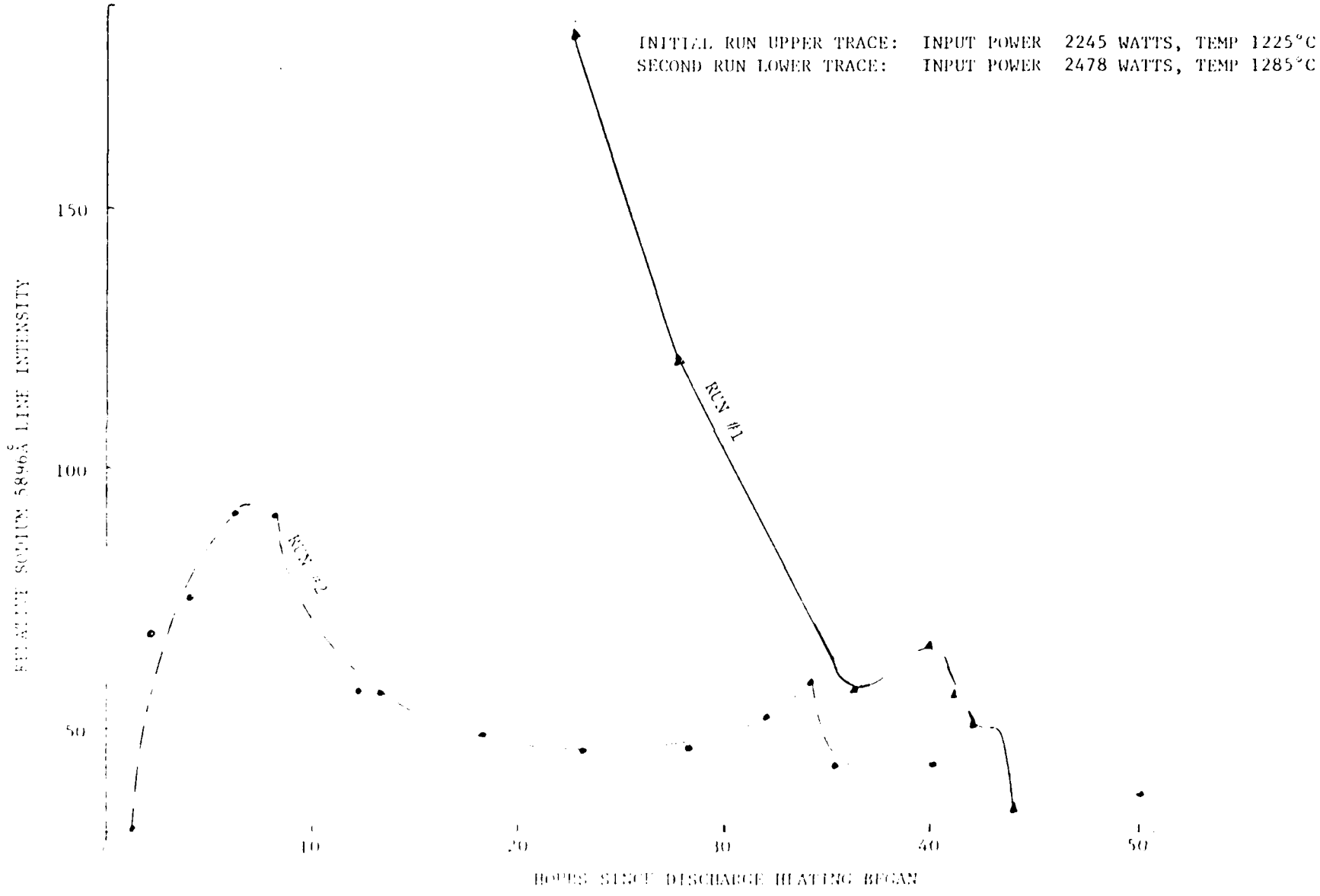

FIGURE 9. SPECTRAL LINE INTENSITY VARIATION
IN COPPER VAPOR LASER: INITIAL HEATING
BUFFER PRESSURE: 4.4 torr HELIUM
REPETITION RATE: 6.25 kHz

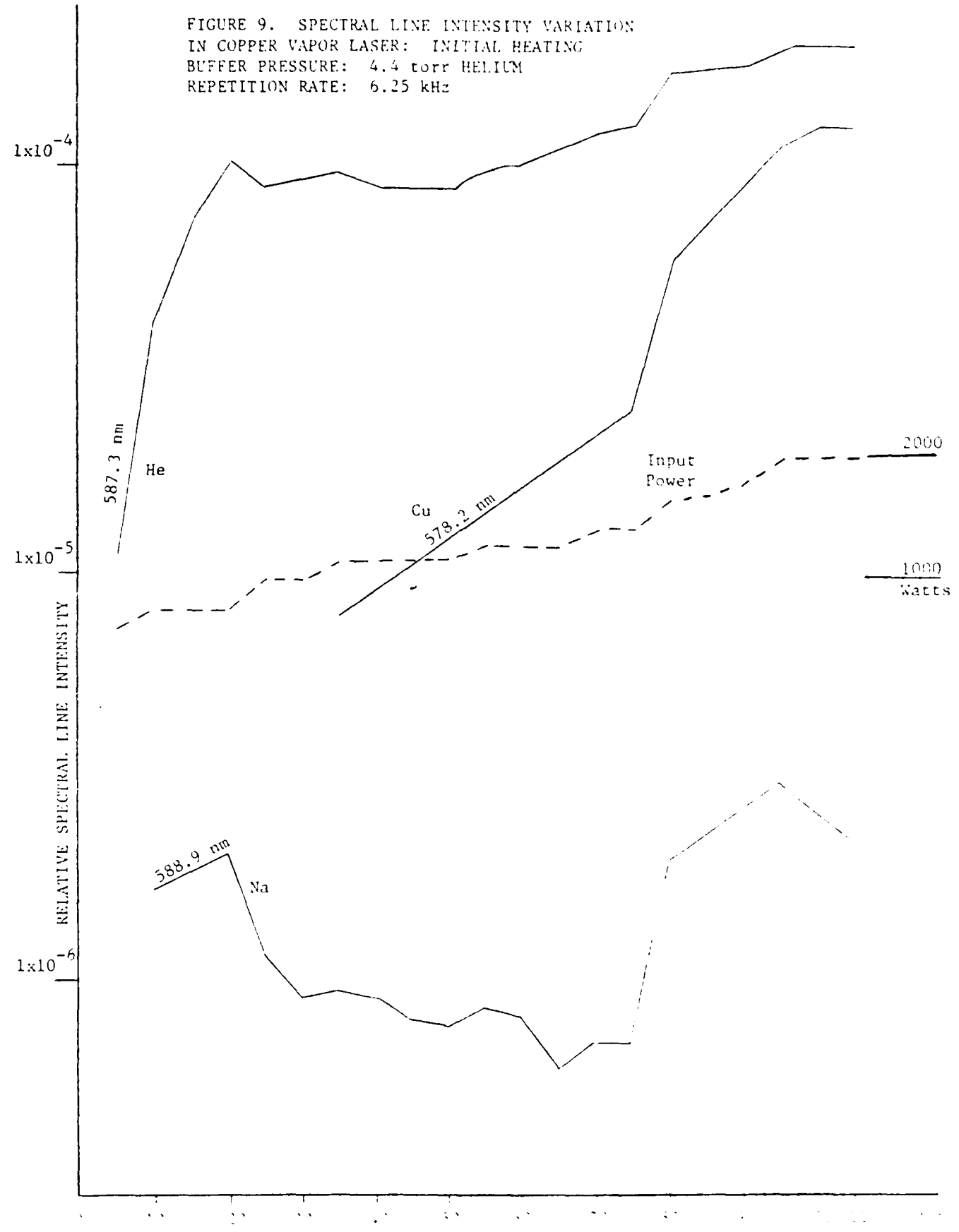

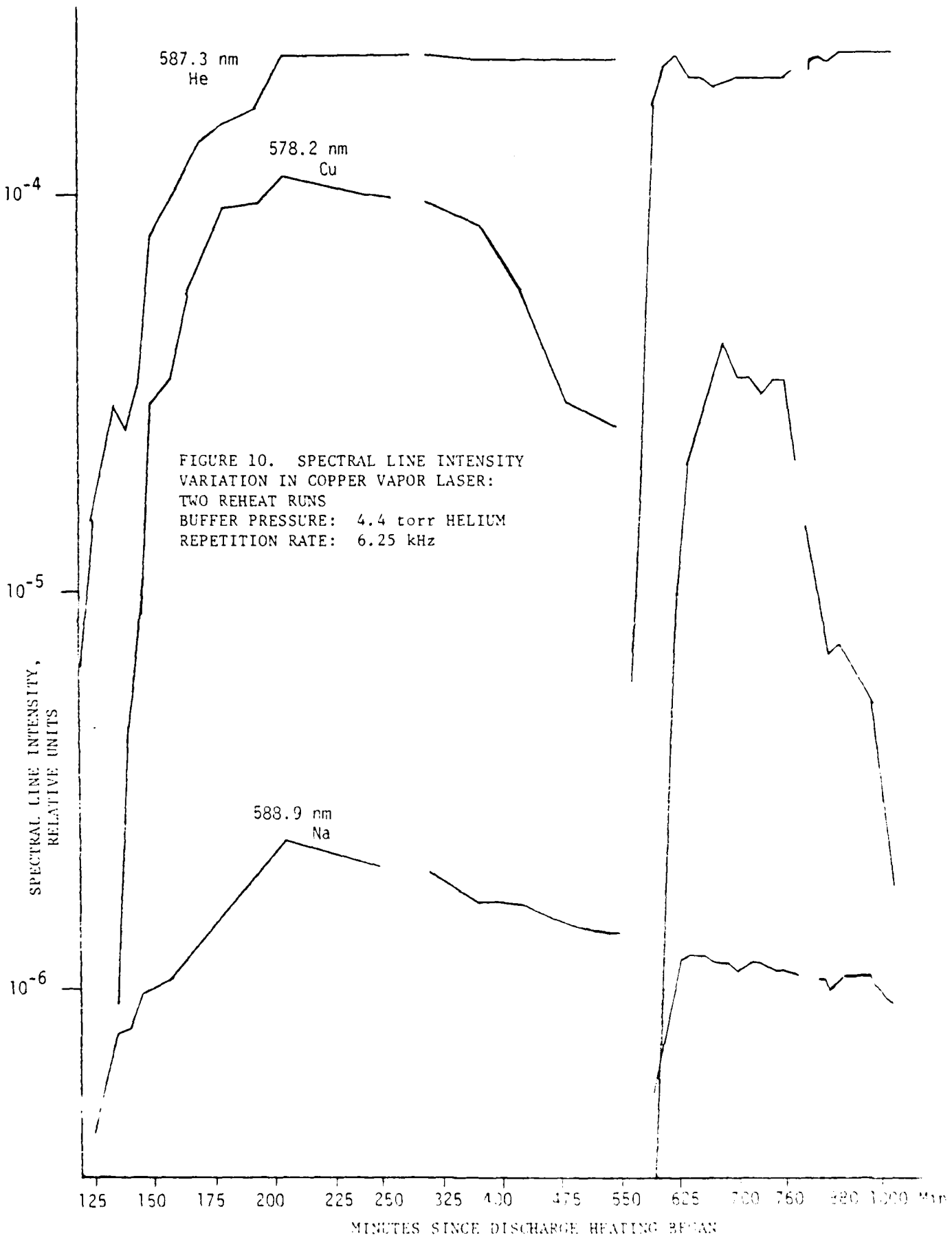

FIGURE 10. SPECTRAL LINE INTENSITY VARIATION IN COPPER VAPOR LASER:
TWO REHEAT RUNS
BUFFER PRESSURE: 4.4 torr HELIUM
REPETITION RATE: 6.25 kHz

Table 8, but different from that shown in Figure 8. Clearly the mechanism controlling sodium loss does not change with temperature but increased temperature may, as in the Case of Figure 8, uncover new sources that temporarily lead to a slower decay or even increase in sodium line intensity.

The decline in copper line intensity in Figure 10 is typical of the behavior of the laser as it runs out of laser metal. At no time does the spectral line intensity of the contaminants decline at such a rate. Evidently there is some fundamental difference between the way the laser metal and contaminant species are delivered to the discharge that causes the depletion of the latter to be slower.

C. Laser Tube Preparation in Aireye Program

GE-ASL is currently designing and manufacturing a lead vapor laser to be used as an illuminator for an airborne Aireye AGTV system.[11] For this particular application the laser tube must either be completely sealed off or at most have extremely low leak rates of buffer gas into the thermal shield region. In order to accomplish this the ceramic laser tube must have metal end caps attached with a vacuum tight braze joint. It is well known that the preparation for brazing of ceramic materials such as these includes many tedious steps designed to ensure meticulously clean surfaces for successful brazing.

However, as described above, the work leading up to and including the current program has demonstrated that these ceramic laser tubes evolve contaminating species into the active zone under the high temperature discharge conditions existing in normal operation. These contaminants must be reduced to ensure satisfactory performance of the laser tubes for long life operation in a sealed-off mode.

As described in the previous sections of this report, long term discharge heated operation of the ceramic tubes at elevated temperatures reduces the contamination levels substantially over the time span of several tens of hours (Figures 6, 7, 9, and 10). Therefore, it was decided to include as an additional step in the ceramic cleaning process a discharge bakeout procedure. This step was inserted prior to the metallization of the ceramic because of the high likelihood that the seals or any unfinished portion of them would not survive the elevated temperatures or exposure to the discharge required for the bakeout.

The bakeout period for each tube was selected to be a continuous interval of 48 hours ($\pm$10%) at a temperature of 1300^{o}C ($\pm$3%). During the bakeout the buffer gas pressure, discharge input power and tube temperature were closely monitored and maintained as constant as possible. The temperature at the center of the tube was measured with a hot filament optical pyrometer.

The data obtained from these bakeout runs is presented in Table 9. As a measure of the clean-up process the relative intensity of the Na 5895.5 angstrom line was continuously recorded throughout the 48 hour bakeout period. The only exceptions to this rule were three of the first tubes processed which had no record during the first few hours of bakeout. For eleven of the sixteen tubes a complete spectral scan from 6500 to 3500 angstroms was taken at the end of the bakeout run. These eleven form the basis for the statistical analysis described below.

As expected, the dominant lines of the tube spectra are from the helium buffer gas. The principal contaminating species were hydrogen and sodium. In addition, in tubes #24 and #18, which were two of the highest in temperature, there were very weak, and hence inconclusive, indications of chromium and magnesium lines. This is entirely consistent with earlier observations that

TABLE 9. TABULATION OF ARGUS TUBE BAKEOUT CHARACTERISTICS

Date	Tube No.	Buffer Pressure P_{He} Torr	Input Power P_{IN} Watts V	I	R	Time to Reach Full Power $t_{Full\ Pwr}$ Min.	Peak Sodium Line Intensity $I_{Pk\ Na}$ Rel.	Time to Peak Sodium Line Intensity $t_{I\ Pk\ Na}$ Min.	Local Minimum In Sodium Line Intensity $I_{Min\ Na}$ Rel.	Time to Minimum in Sodium Line Intensity $t_{I\ Min\ Na}$ Min.	Sodium Line Intensity at End of Run $I_{end\ Na}$ Rel.	Helium Line Intensity at End of Run $I_{end\ He}$ Rel.	Hydrogen Line Intensity at End of Run $I_{end\ H}$ Rel.	Tube Temp. at End of Run T_{end} °C
3-31 to 4-02-80	10	19.5	4.5	295	.0151	55	49	65	18	160	17	9.5	16.5	1305
			1328											
3-26 to 3-28-80	2	19.5	4.5	290	.0155	45	72	80	28	220	23	12	7.5	1305
			1305											
3-25 to 3-26-80	6	21.0	4.5	295	.0151	50	>100	<60	49	220	43.5	38.5	41	1315
			1328											
3-19 to 3-25-80	24	21.0	4.5	295	.0151	50	110	60	44	200	43	43	68	1325
			1328											
3-17 to 3-18-80	18	23.0	4.5	298	.0151	50	110	65	55	120	50.5	39	61	1310
			1341											
3-13 to 3-14-80	12	21.0	4.5	295	.0151	45	>100	65	49	155	46.5	23	10	1310
			1328											
3-10 to 3-12-80	14	20.0	4.4	288	.0153	70	130	85	40	175	32	34	61.5	1300
			1267											
3-05 to 3-07-80	4	20.5	4.4	292	.0151	100	130	50	66	200	52.5	59.5	45	1300
			1285											
2-22 to 2-25-80	1	25.2	4.4	290	.0152	80	>100	80	62	280	45	-	-	1320
			1276											
2-19 to 2-21-80	8	21.0	4.42	290	.0152	80	>100	70	11	220	11	44	26	1280
			1282											
2-14 to 2-15-80	15	15	4.55	290	.0153	120	33	80	15	150	15	-	-	1280
			1291											
2-11 to 2-13-80	3	22.5	4.33	287	.0151	120	-	-	17	<210	15	41.5	47	1265
			1243											
2-07 to 2-09-80	9	17.5	4.4	290	.0152	110	-	-	5	220	5	-	-	1280
			1276											
2-05 to 2-06-80	11	21.0	4.35	280	.0152	110	>100	120	30	210	20	58.5	11	1300
			1190											
2-01 to 2-04-80	13	19.2	4.38	280	.0154	120	120	160	53	210	50	-	-	1325
			1199											
1-31 to 2-01-80	7[1]	18.0	4.4	280	.0154		-	-	-	-	16	-	-	1235
			1205											

[1] Tube #7 run data is not available.

The Argus tube used in the above test, were different from those used in other parts of this report and quantitative comparisons of physical characteristics from this table to other tables or figures should be avoided.

show the spectral lines of these elements to be clearly in evidence in scans of copper laser tubes (1400°C) and be essentially absent from lead laser tubes (900°C).

The principal interest in the sodium line intensity is as an indicator of the tube contamination and its time dependence. From the table it can be seen that the sodium line intensity reaches a peak value within 60 to 120 minutes (t_{I-Pk} in Table 9) after turn on. As expected, there is a correlation between the time to peak intensity and the turn-on sequence. That is, the longer the elapsed time from turn-on to reach a given full input power ($t_{Full\ Pwr}$ in Table 9), the longer the time to peak sodium intensity. A lower peak input power will also extend the time required to reach peak intensity.

Once the peak is reached the intensity falls to a minimum value which is typically a factor of 2 to 3 lower. This occurs over a period varying from about 1-1/2 to 4-1/2 hours. In over three-quarters of the tubes this minimum value was within 20% or less of the final sodium intensity level at the conclusion of the 48 hour soak period. These results are qualitatively in agreement with those shown on Figures 8 and 9.

The data from the eleven complete spectral runs have been analyzed in more detail. The tube temperature during processing shows only a moderate positive correlation ($r = +0.58$) with input power rather than the strong relation one might expect. Similarly, the final sodium line intensity was found to have only a moderate positive correlation ($r = +0.65$) with the tube temperature. The increased vapor densities which accompany increased temperature would be expected to produce higher line intensity.

Part of the reason for this discrepancy may lie with variation in the

initial contaminant concentration within the ceramic tube walls. None of the tubes run between 2/19/80 and 4/2/80 (see Table 9) were operated with a higher input power than was tube #10 but all produced higher initial peak sodium line intensity. This low sodium line intensity characteristic continued throughout the life of that tube. Similar low sodium character was true for tube #15 and to a lesser degree tube #2.

This variability of sodium line intensity for the group of tubes studied was about 50%-80%. Comparison of tubes #11, 13, and 7, which had about the same input power (±0.6%) and buffer pressure (±7%), shows such a variation, as does any group of similar tubes (see Table 10). The possibility of such a variability from tube to tube has also been confirmed by the supplier.[12]

This variability shows up in a practical way when one seeks to establish how long a given tube must be baked to reduce impurity line intensities in a given amount. The tubes in Table 9 had sodium line intensity that decreased anywhere from more than a factor of ten to about a factor of two, though they were discharge-heated under similar conditions. It is consequently difficult to determine when contaminant levels have fallen sufficiently without directly monitoring their line intensities during the course of discharge-heated bakeout.

A more marked example of discharge tube variability can be found by contrasting the decay of contaminant line intensity found with those tubes to the decay found with others investigated on this program (e.g., Figures 6 and 7). The early experiments usually had peak sodium line intensities [illegible] on the scale of Figure 7 and long term intensities of about 10-30 on that scale. The Aireye bakeout runs, using the same spectral monitoring system and presumably the same sensitivity scale, had peak sodium line intensities of

TABLE 10

COMPARISON OF SODIUM LINE INTENSITY
AT END OF RUN FOR TUBES OPERATING
UNDER SIMILAR CONDITIONS

	Tubes Compared	Max % Variation In Buffer Pressure From Mean	Max % Variation In Input Power From Mean	Max % Variation In Sodium Line Intensity From Mean
Low Power	11,13,7	7%	.6%	77%
Mid Power Mid Pressure	14,4,8	2.4%	.9%	63%
High Power	10,6,24,12	5%	0	53%
Low Pressure	9,15,2	13%	1.1%	63%
High Pressure	18,1,3	9.6%	4.2%	50%

100-150 and 10-50 after their bakeout.

Evidently there is a considerable difference between the two sets of data. However, the difference lies in substantially lower initial peak sodium line intensities with the Aireye tubes. The sodium line intensities after bakeout were comparable.

A batch to batch variability in the sodium conrent in ceramic tubes, that exceeds the tube to tube variability within a given batch, is indicated. For instance, the variability in the batch described by Table 9 is about 50% while it is a factor of ten between this batch and those used in Figure 7.

VII. WICK CLEAN UP

The preceeding studies have shown no marked spectral dependence upon the presence of wicks. This is due to the total absence of tungsten and tantalum from the spectra and a primary interest on the latter stages of bakeout. However, the presence of wicks does affect contaminant evolution during the early stages of laser operation.

The addition of wicks to a laser, before they have been loaded with laser metal, greatly increases the surface area available for adsorption of hydrocarbons, atmospheric species, and other contaminants. Consequently, the time required to reach a given level of spectral intensity is extended but only for a few tens of hours. Beyond that period contaminant evolution proceeds much as before. Evidently contaminants absorbed within the wick material play a negligible role.

This can be best seen by noting what happens during a process in which the ceramic tube and tube wick assembly are heated sequentially. This has been done with a number of 1 1/4" ID tubes destined to be lead vapor lasers. The decline in sodium intensity was generally similar to that shown in Figure 7. The sodium 5889A line intensity attained after discharge heating the ceramic alone was generally the order of 12.5-15 on that figure. Subsequent baking with wicks inserted brought the sodium intensity down to about 10-11 on the same scale. These results indicated, and have since been confirmed, that approximately two days (48 hours) of discharge heating, with or without wicks, will produce the same line intensity as a long run. In contrast, the addition of laser metal to the wicks before they have been well baked out leads to incomplete wetting and slowing of contaminant evolution. The most startling observation,

associated with outgassing of the wick through the laser metal, is the appearance of bubbling and similar movements of that liquid. Inadequate preheating of laser wicks will thus always be evident.

While gross contamination of wicks was generally cleaned up before laser metal was added, small levels of contaminants were more difficult to observe. Wetting may be adequate and bubbling of the liquid metal may not be observed but there can still be an effect on long term wick operation.

Appendix 3 describes two sets of experiments using discharge preheating of lead vapor laser wicks as a parameter. One set used only limited heating before lead was placed in the wicks. The other set used wicks that were preheated at least 20 hours. Figure 1 of Appendix 3 shows that the preheated wicks consistently contained the lead vapor longer. The difference was as much as a factor of 4 with clean conditions leading to lifetimes of several hundred hours. The longest test on this program, and we believe anywhere with a lead vapor laser, was over 300 hours.

The difference is related to the wetting of the liquid metal on its wick and, possibly, the cleanliness of the liquid metal surface. A contaminated wick will not be wet well by the liquid metal and, with passing time, the wetting forces will decline. This results in a decline in the flow of liquid back into the hot zone. Eventually there will be an imbalance between the metal vapor lost to the cool end of the wick and that return flow of liquid. The deficit will accumulate until the wick is dry in spots and flow is interrupted. The vapor within the hot zone is not replenished and a precipitous drop in laser power results.

Often the loss of wetting will be so sudden that drops of liquid metal will form on the wick, usually at its cool end. Vapor lost from the hot zone will accumulate here blocking the laser beam.

As an aid in the cleanup process, a small quantity of hydrogen was sometimes added to the buffer gas. Oxides and other contaminants were more quickly reduced. Furthermore, if laser metal was added to a wick later found to still be contaminated, the addition of hydrogen was by far the fastest way to get wetting to take place. Of course elevated levels of hydrogen could be found in the laser tube for some time but this rarely had a long term impact upon the laser output.

The laser lifetime data in Appendix 3 are presented using a dimensionless parameter found to fully characterize the wick: the length to diameter ratio. The laser lifetime dependence is of the form:

$$T = \frac{S}{F_o} \exp\left(-K' \frac{\ell}{d}\right)$$

where S is the amount of metal stored, F_o is the vapor loss rate for zero wick length, ℓ, is the wick length, d its diameter and k' a constant. A model is presented to explain this dependence.

The general applicability of the formulation is emphasized in Figure 1 of Appendix 3 through the inclusion of long life data from another program using copper vapor lasers. Thus, while the range in lifetime data used in that figure is the order of a few tens to several hundreds of hours with lead and copper lasers, there is every reason to believe that the model can be extended well into the range of several thousand hours.

VIII. FURNACE HEATING

The studies discussed in the previous section have indicated that the primary source of contaminants is a thermal mechanism which "cleans up" contaminants in the alumina ceramic of the discharge tube. In order to confirm this a series of experiments were conducted using a furnace to heat the tube. In this way the heating could be limited to the ceramic and discharge mechanisms could be eliminated as a contributing factor to any contaminant clean-up.

Two 24" long lead laser tubes were preheated. One was heated in a muffle furnace with a tempeiature distribution as indicated on Table 11. It was held at this maximum temperature for 48 hours. The second tube had been discharge-heated extensively (~100 hrs.) at temperatures below 1250°C and in preparation for these tests was heated to 1285-1290°C for 32 hours.

Both tubes were then run with the same 8" long thermal shield and under the same discharge conditions. Full spectral scans were taken several times during the course of each run.

Such a short hot zone was chosen so that the essentially unheated ends of the furnace baked tubes would not be subjected to elevated temperature. Obviously it would have been preferable if the furnace baked zone had been just as long as that discharge-heated but, a furnace of appropriate length and temperature was not available.

A comparison of spectral line variation for tubes prepared in both ways is shown on Figures 11-14. Figure 11 shows that both tubes ultimately reached about the same input power and tube temperature. The furnace heated tube just lagged by about 1/2 hour.

TABLE 11

BAKING TEMPERATURE PROFILE OF MUFFLE FURNACE
HEATED CERAMIC TUBE

DISTANCE FROM CENTER - INCHES	TEMPERATURE °C
0	1370
3"	1330
6"	1060
12"	330

FIGURE 11. COMPARISON OF INPUT POWER AND DISCHARGE TUBE TEMPERATURE DURING STANDARD LEAD LASER RUN. TUBES PREPARED BY DISCHARGE HEATING OR FURNACE HEATING.

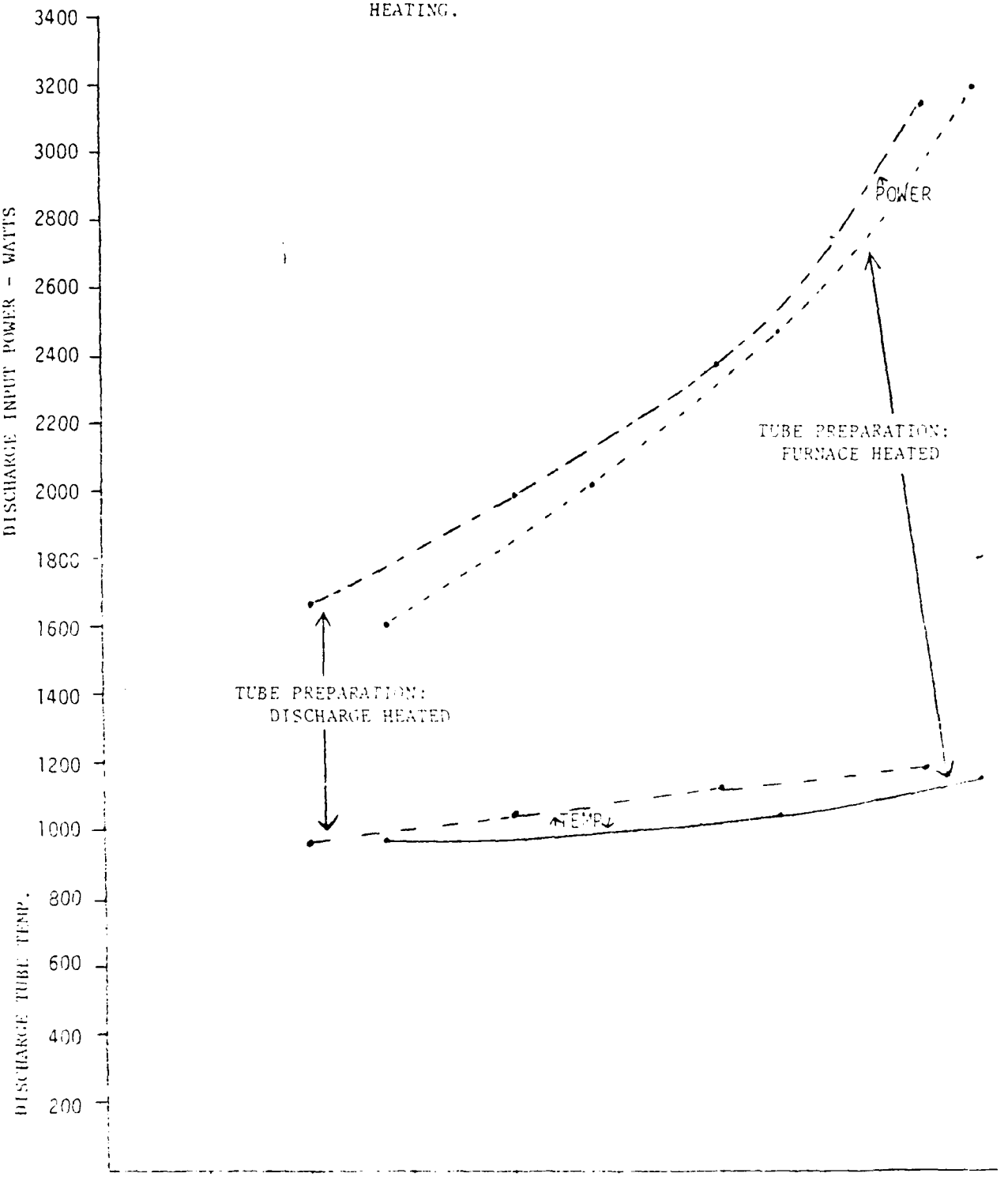

FIGURE 12. COMPARISON OF HYDROGEN 4314Å AND OXYGEN 5331Å LINE INTENSITY DURING STANDARD LEAD LASER RUN. TUBES PREPARED BY FURNACE HEATING OR DISCHARGE HEATING.

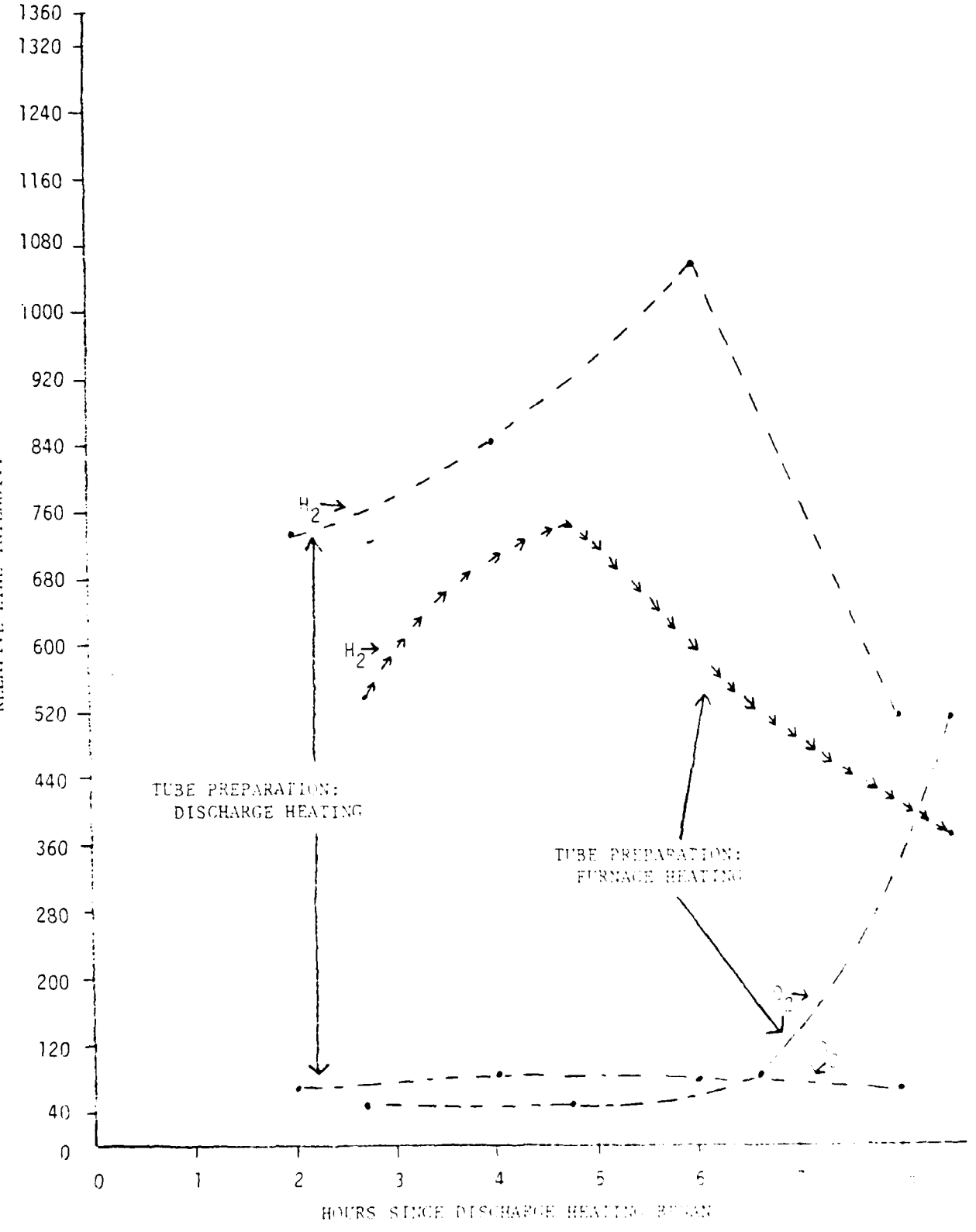

FIGURE 13. COMPARISON OF CALCIUM (4435Å) AND NITROGEN (5374Å) LINE INTENSITY DURING STANDARD LEAD LASER RUN. TUBES PREPARED BY FURNACE HEATING OR DISCHARGE HEATING.

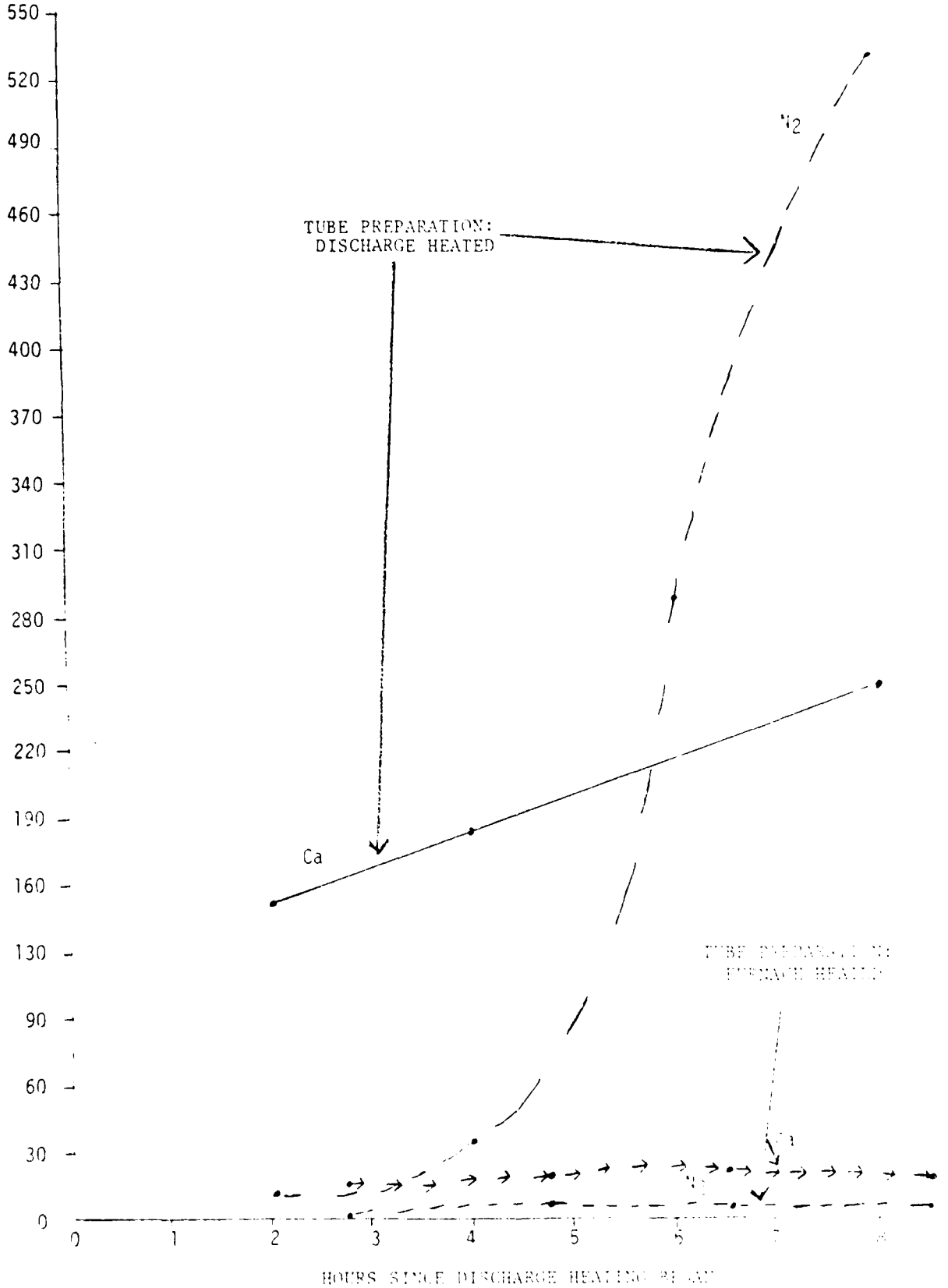

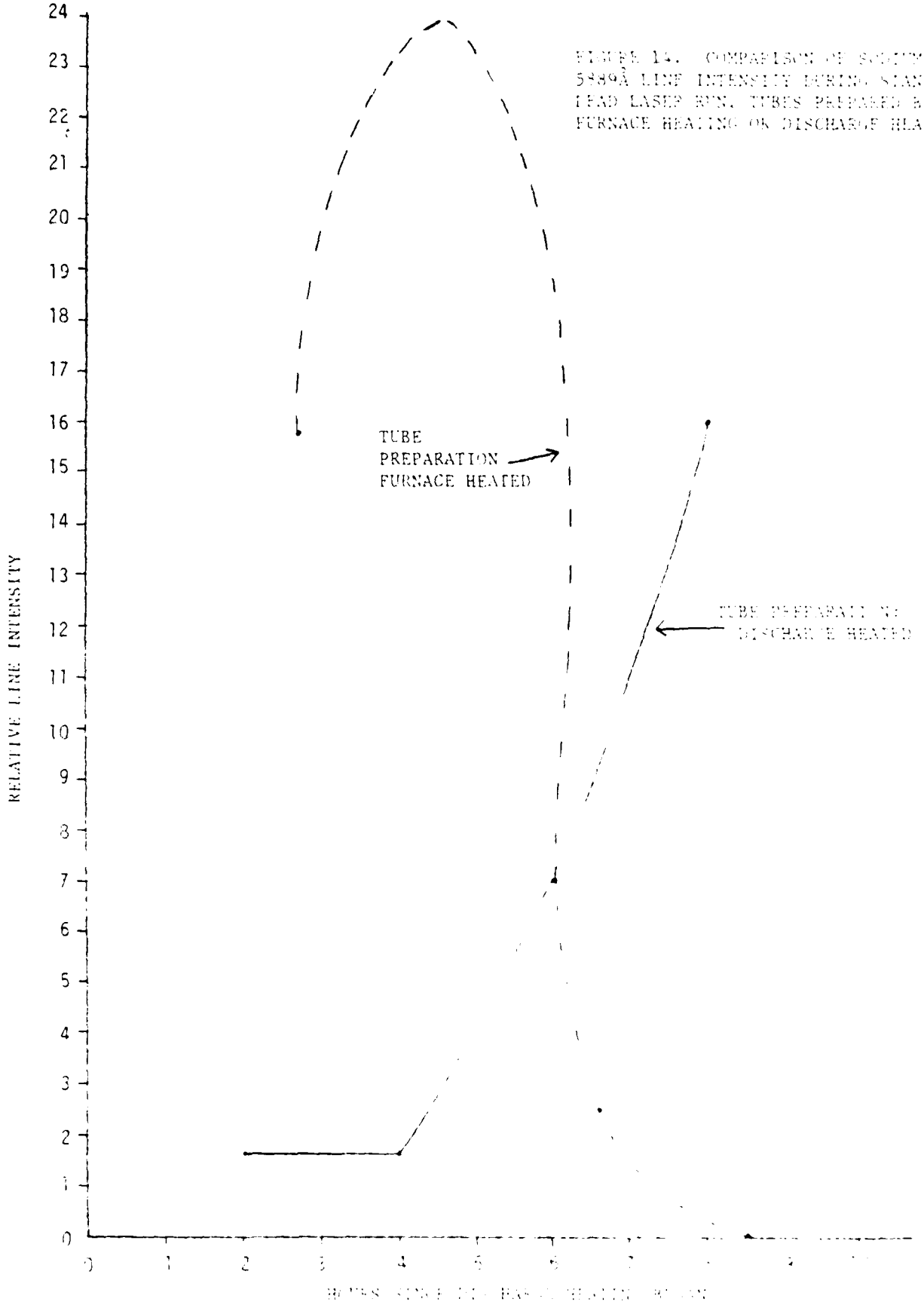

FIGURE 14. COMPARISON OF SODIUM 5889Å LINE INTENSITY DURING STANDARD LEAD LASER RUN. TUBES PREPARED BY FURNACE HEATING OR DISCHARGE HEATING.

Generally, the furnace heated tube was more free of contaminants than that prepared by discharge heating. Hydrogen (Figure 12), nitrogen and calcium (Figure 13) line intensities were lower throughout the course of the runs. Sodium line intensity from the furnace heated tube began very high but quickly fell to indetectably low levels. Only the oxygen line intensity was higher for the furnace heated tube than for the discharge-heated tube. Clearly furnace heating is at least as effective in cleaning out contaminants as is discharge heating.

In order to extend the use of furnace heating in temperature and dimension, two ceramic tubes (for use in a standard copper vapor laser) were sent to the General Electric Lamp Glass Department in Cleveland, Ohio to utilize a production line furnace for Lucalox lamps that heats ceramic tubes to 1800°C for 48 hours. In this furnace all parts of the tube are brought up to 1800°C.

After processing these tubes were run under typical copper laser discharge conditions with input power gradually increasing throughout each run. As in most such runs, the rate at which power was increased was determined by the cleanliness of the tube light output. An untreated tube was run in the same way for comparison. Records of the sodium 5895 angstrom spectral line intensity is given in Figure 15.

It can be seen that the untreated tube, which could only be brought up to 1520 watts input in this time without undue discharge instability, has sodium line intensity that lies highest. A second reheat cycle with copper added could be brought to 1722 watts input and produced a modest reduction in sodium line intensity. A greater reduction was not observed because of the brevity of the first heat up cycle. Long term discharge heating could reduce line intensities down to the 10^{-6} scale level (see Figure 9).

FIGURE 15. COMPARISON OF SODIUM 5895Å LINE INTENSITY DURING COPPER LASER RUN. TUBES EITHER UNPREPARED (TWO SUCCESSIVE RUNS) OR HEATED IN 1800°C FURNACE (TWO SUCCESSIVE RUNS)

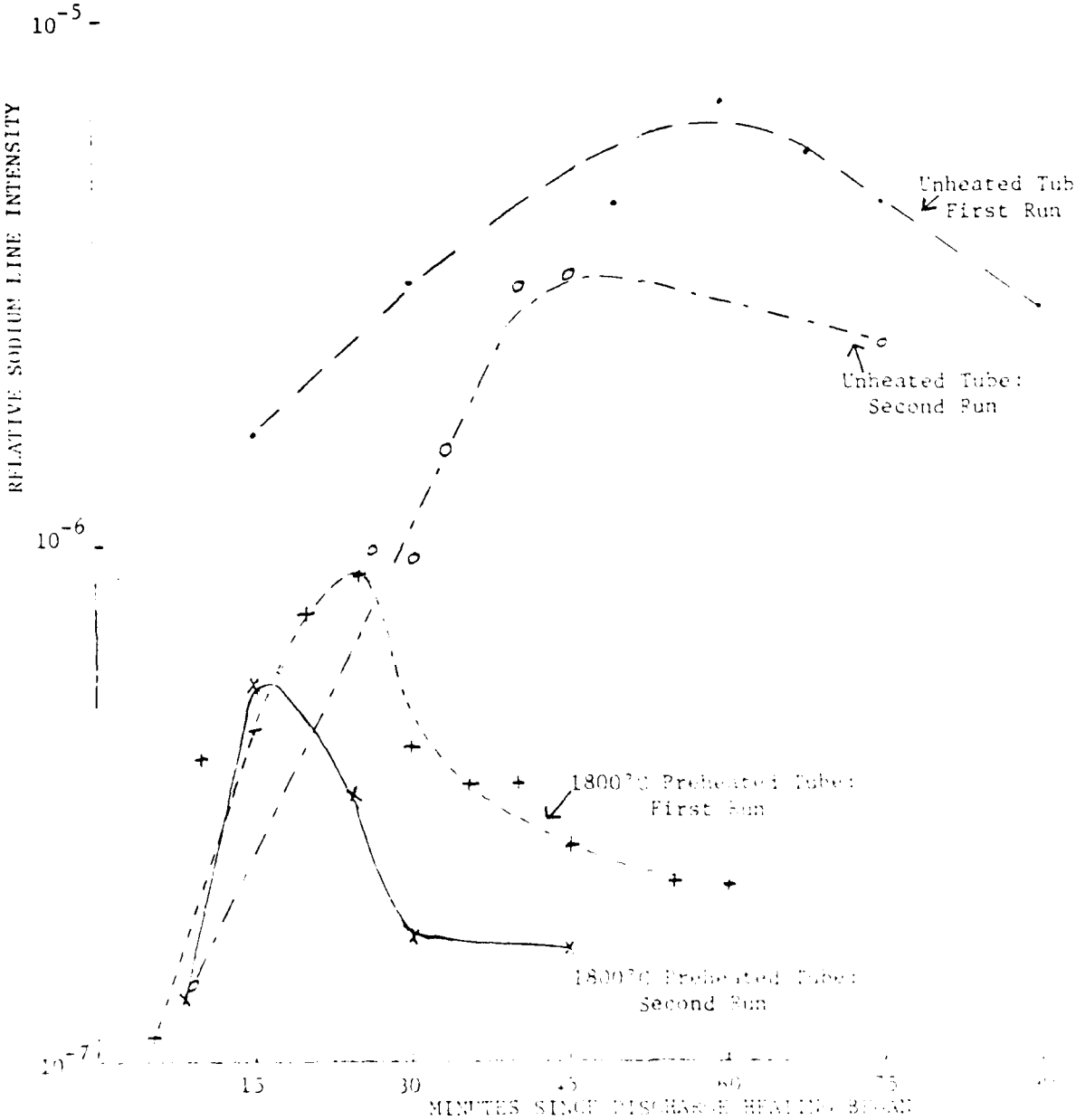

In contrast, a tube preheated to 1800°C in Cleveland could be brought up to 1845 watts input, almost standard operating conditions, with only weak evidence of contamination. The peak sodium line intensity was as low as could be obtained only after long term operation with any other tube. Furthermore, the sodium line intensity fell very rapidly from this peak, implying a superficial source that is quickly depleted. A second run had the same form except at even lower values of sodium spectral line intensity and faster fall off. The input power was 1935 watts and the laser power 4.5 watts. It is interesting to note that the sodium line intensity was essentially constant after its fall at the 30 minute mark despite an increase in input power from 1420 watts to 1935 watts.

Clearly furnace preparation of the alumina ceramic is sufficient to provide the contaminant clean-up desired.

IX. SEALED OFF LASER OPERATION

During the course of this program a sealed-off lead laser was tested in order to evaluate the effects, if any, due to the build-up of contaminating species over a long-term, during which they were not flushed out with a buffer gas. A description of the laser is included in Appendix I.

The laser was baked for 106 hours. The first 48 hour bakeout, similar to those done previously, used a flowing buffer (24 hours at 1100°C and 24 hours at 1200°C). Sodium line intensity at the end of this bakeout was 10 on the scale of Figure 7. Oxygen 5331A line intensity was stable. A new sequence was then added in which the window assemblies and windows were heated as well as the discharge tube. During this process the windows were heated to over 200°C and the discharge tube to 1270°C for almost 4 hours.

Most contaminant lines were not observable (10 on scale of Figures 6 and 7). Only nitrogen, oxygen and hydrogen could still be seen. However, after being sealed off and run for six hours, nitrogen, oxygen and hydrogen atomic lines decreased by a factor of two or more while some of their molecular lines began to appear. Simultaneously the total (helium) pressure fell at a rate of 0.23 mm/hr. This pressure decrease continued throughout a comparable run taking place during the next day. The rate was then 0.21 mm/hr, producing a net helium pressure drop of 2.8 mm or 23% of the 12.3 mm fill.

At this point the laser was opened and lead was added in preparation for lasing. The shell was filled with helium and the lead was melted into the wicks while the laser was in a flowing condition. In this way any contaminants evolved from the lead were carried off by the flowing helium buffer gas. By the end of this last bakeout the 106 hours mentioned before had been accumulated.

During the sealed off run described in Appendix I, both pressure measurements and spectral scans were continued.

The spectral line scans were generally quite simple with no clear evidence of calcium, oxygen, or most other chemically active impurities. Similarly, there was no indication of molecular bands or similar complex line formations. Only helium, lead, and hydrogen were strong and nitrogen and sodium could be identified. At no time, short of vacuum failure, did the intensity of any of these lines increase. This encompassed a sealed-off period of 108 hours during 70 hours of which the laser was in operation.

This result is particularly significant since it shows that gas evolution had been minimized, if not eliminated, by the previous bakeout. Furthermore, the saffil and zirconia insulation surrounding the laser tube, and now also within this same sealed region, are compatible with the temperature and pressure ranges used.

The intensities of contaminant spectral lines not only did not increase, they declined at a rate of about 20% in 21 hours (Table 12). During the same time the total pressure fell from 22 mm to 20 mm or 10% in 21 hours. This was accompanied by an increase in discharge tube temperature (890°C-915°C) and laser power output (0.23 W to 0.31 W). Lead spectral lines competing with the upper state of the laser transition fell, as one would expect (see Appendix 4).

The decreasing line intensities and pressure must represent a real decrease in concentration, possibly due to discharge pumping of ions into the electrode.

TABLE 12

DECLINE OF SPECTRAL LINE INTENSITY
OVER 21 HOUR SEALED-OFF RUN

ELEMENT	LINES AVERAGED	% DECLINE
Nitrogen	5005Å	25%
	5379Å	
	5999Å	
	6008Å	
Helium	3889Å	23%
	4713Å	
	5016Å	
Hydrogen	4341Å	20%
	4719Å	
	4861Å	
Sodium	5896Å	24%
Lead	Lines competing with laser transition	23%
	3640Å	
	3683Å	
	4057Å	
	Lines not competing with laser transition	1%
	3740Å	
	4020Å	
	5042Å	

X. MASS SPECTROMETRY

An investigation of the gases within the laser was also conducted with a mass spectrometer. The dominant peaks observed and their identification is given in Table 13.

For reasons that are not understood, hydrogen was never seen. Otherwise all the non-condensible atomic constituents identified in the optical spectra were observed. Some of the molecular species found in these studies were also seen in the optical spectra but others (CO_2 and H_2O) were not. Nitrogen was always the dominant contaminant.

Major difficulties were encountered in attempting to obtain a quantitative calibration of contaminant concentration from this data. The presence of r-f fields and the high pressure inert gas buffer caused particular difficulties. Consequently, other techniques were used to obtain calibration estimates and the mass spectrometry results only supplemented our knowledge of which trace contaminants were present.

TABLE 13

LIST OF SPECIES FOUND WITH
MASS SPECTROMETER*

SPECIES	MASS (amu)	
He	4	F
C	12	S
N	14	M
O	16	S
(NH_3 or OH)	17	S
H_2O	18	S
Ne	20	F
	22	S
N_2	28	M
O_2	32	S
A	40	S
CO_2	44	S

*Note that helium and neon buffer gas was used during these tests.

Key:

F denotes buffer fill gas

M denotes major contaminant

S denotes small contaminant

XI. ABSOLUTE CONCENTRATION OF CONTAMINANTS

In order to obtain an estimate of contaminant densities a series of measurements were performed in which the partial pressure of one or more species was varied during a series of optical spectral scans. The sealed off laser discussed in Section IX and Appendix 1 was ideal for such a purpose since a given gas pressure and composition measured outside of the hot tube could be used to establish the pressure within that discharge tube.

The analyses to be discussed here involved a small leak to atmosphere and periodic pressure measurements over long periods (e.g., 13 to 95 hours) to establish impurity concentrations. In this way impurity levels of hydrogen and nitrogen were added. The nitrogen (N_2) partial pressure was always taken to be 78% of the atmospheric pressure admitted. The hydrogen (H_2) partial pressure was largely the product of water dissociation* and so was taken to be 1.47% of the atmospheric pressure admitted (18.65 mm water vapor pressure at 21°C x 60% relative humidity).

The spectral measurements were referred to the intensity of a helium line so that small differences in alignment, etc. could be accounted for. The dependence of such scaled line intensities on the partial pressure of the constituent is linear. Figure 16 shows this linearity for two lines of nitrogen and one of hydrogen. Since the lines extrapolate to the origin this calibration can now be used to estimate the partial pressure of nitrogen or hydrogen from

*The discharge used was of such an intensity that nitrogen molecular bands were very small and no other molecular bands could be found. In addition, the corresponding atomic lines were strong, implying that molecules with dissociation energy less than that of nitrogen (9.7 eV) must be fully dissociated. Since the OH dissociation energy is only 4.35 eV total dissociation of water can be assumed.

FIGURE 16. CALIBRATION OF NITROGEN AND HYDROGEN LINE INTENSITIES.
DISCHARGE TUBE TEMPERATURE: 740°C, HELIUM PRESSURE: 18 torr

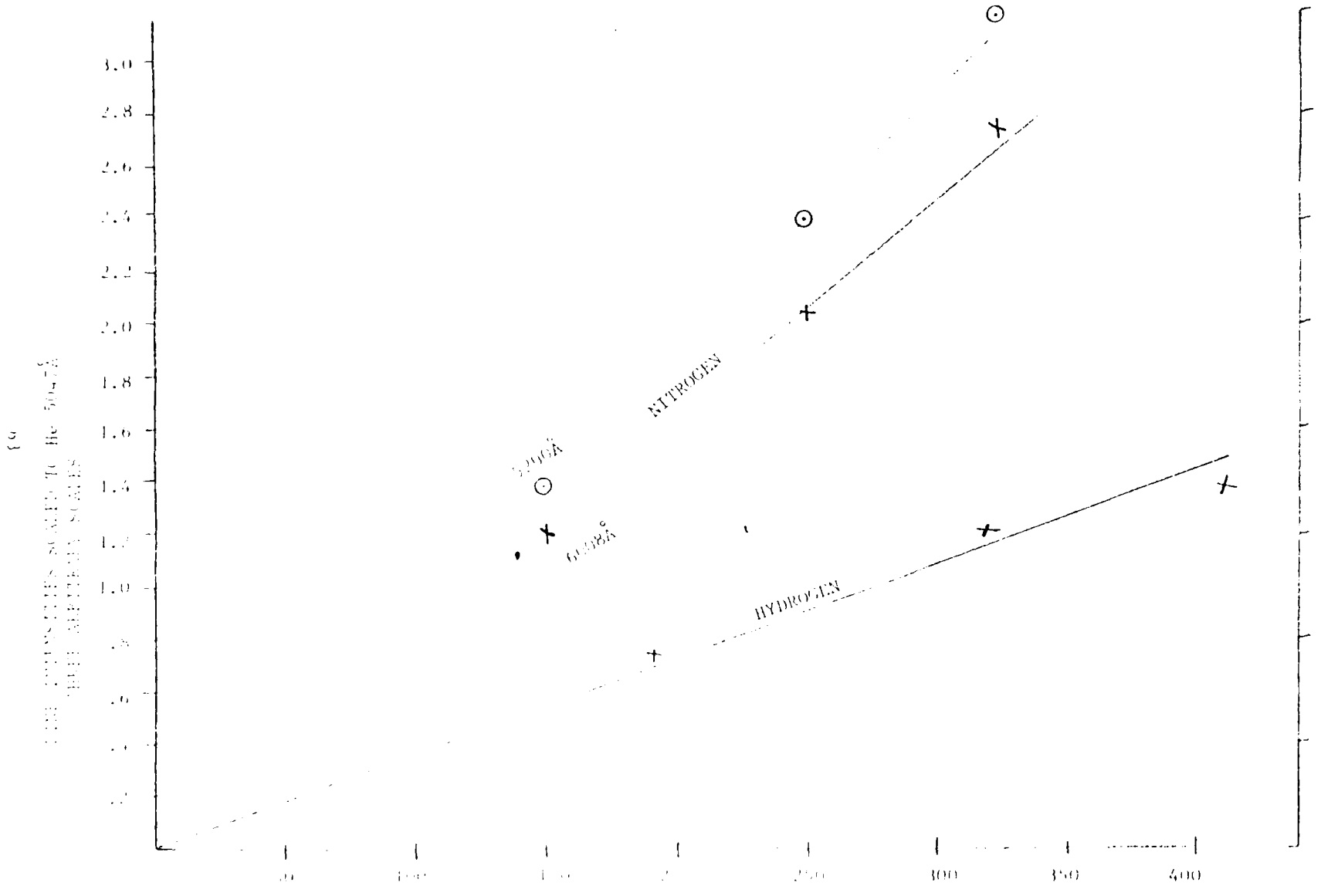

line intensities emitted from another tube operating under similar conditions.

The densities for other species can be estimated if the effective electron temperature is known. The intensity of a spectral line is given by:[13]

$$I = \frac{N}{u} \frac{8\pi^2 e^2 h}{m} \frac{gf}{\lambda^3} e^{-E/kT} \qquad (1)$$

where: I is the intensity

N is the number density

h is Planck constant

E and m are the charge and mass of the electron

λ is the emitted wavelength

E and g are the energy and statistical weight of the upper level of the transition

f is the oscillator strength

k is the Boltzmann constant

T is the electron temperature

and $u = \Sigma_n g_n \exp(-E_n/kT)$ is the partition function for a given species summed over its energy levels.

If the above is solved for:

$$C = \ln \frac{I\lambda^3}{gf} = K - \frac{E}{kT} \quad ,$$

where K is now a constant for the specific species and density, the temperature can be determined by plotting C against E for a number of lines of the same species and finding the slope $kT = \frac{\Delta E}{\Delta C}$. This has been done for helium, nitrogen, hydrogen, and lead vapor in Figures 17-20. The scatter in the data can be related to changes in laser operating conditions during the spectral scan. Two separate groups of data points producing very similar slopes

FIGURE 17. LOG RATIO OF LINE INTENSITY x λ^3 TO gf - VALUE FOR LINES OF HELIUM I PLOTTED AGAINST UPPER LEVEL ENERGY IN A LEAD VAPOR LASER DISCHARGE. AN ELECTRONIC STATE TEMPERATURE OF 1,300°C IS DERIVED FROM THE SLOPE OF THE LEAST SQUARES FIT LINE.

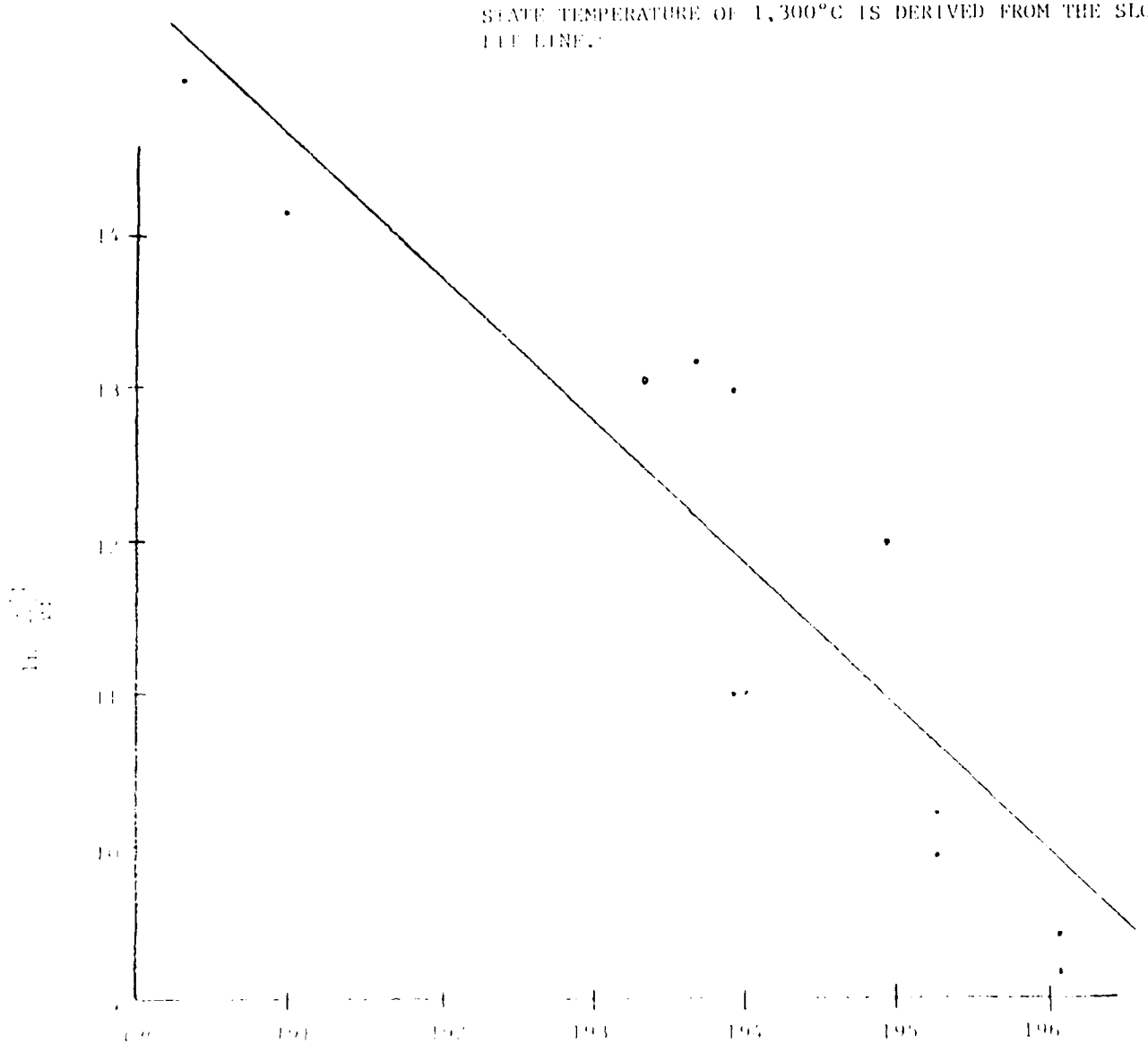

FIGURE 18. LOG (I λ^3/gf) OF LINE INTENSITY x λ^3 TO gf - VALUE FOR LINES OF NITROGEN I PLOTTED AGAINST UPPER LEVEL ENERGY IN A LEAD VAPOR LASER DISCHARGE. AN ELECTRONIC STATE TEMPERATURE OF 1,700°C IS DERIVED FROM THE SLOPE OF THE LEAST SQUARES FIT LINE.

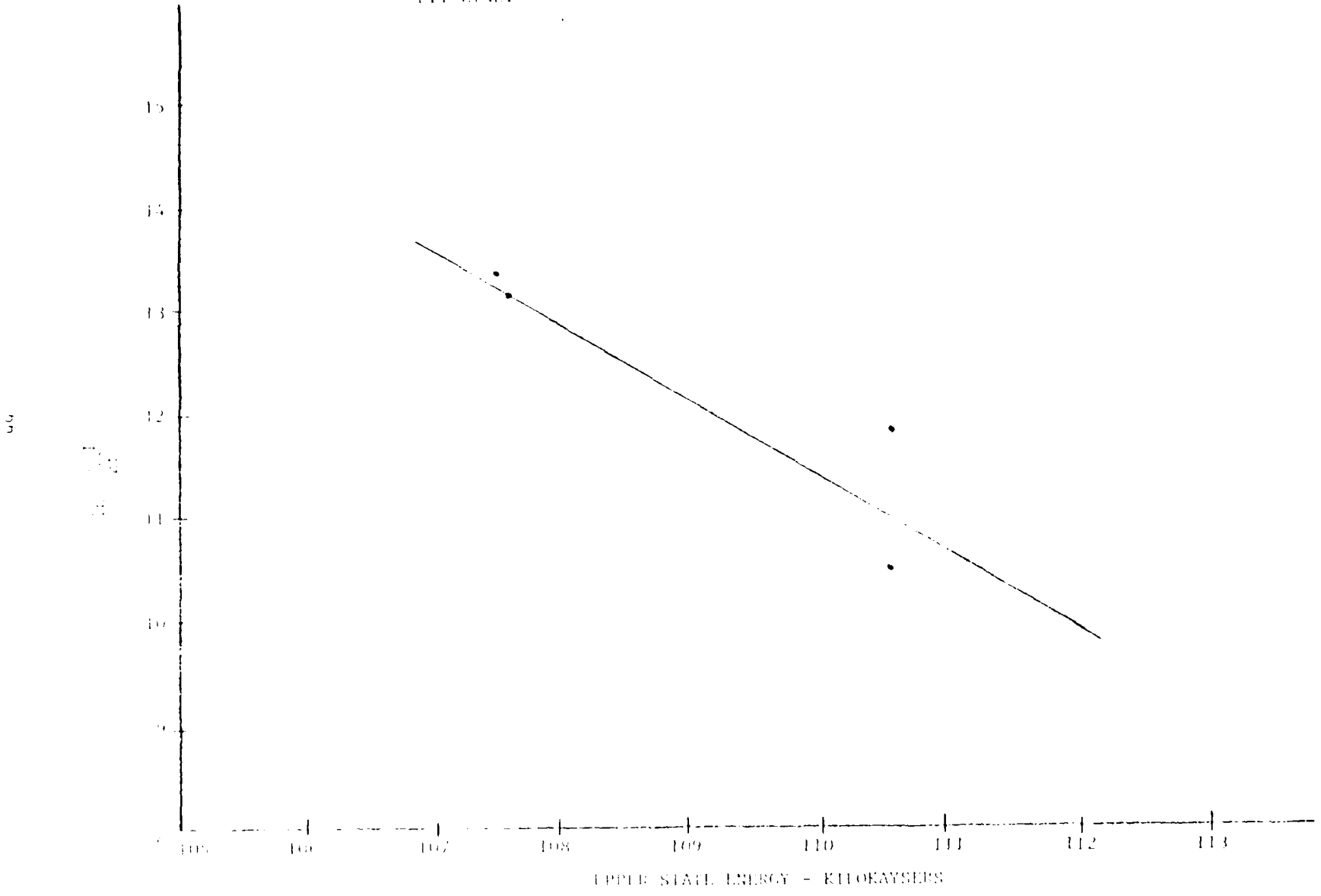

FIGURE 19. LOG RATIO OF LINE INTENSITY x λ^3 TO gf - VALUE FOR LINES OF HYDROGEN I PLOTTED AGAINST UPPER LEVEL ENERGY IN A LEAD VAPOR LASER DISCHARGE. AN ELECTRONIC STATE TEMPERATURE OF 1800°C IS DERIVED FROM THE SLOPE OF THE LEAST SQUARES FIT LINE.

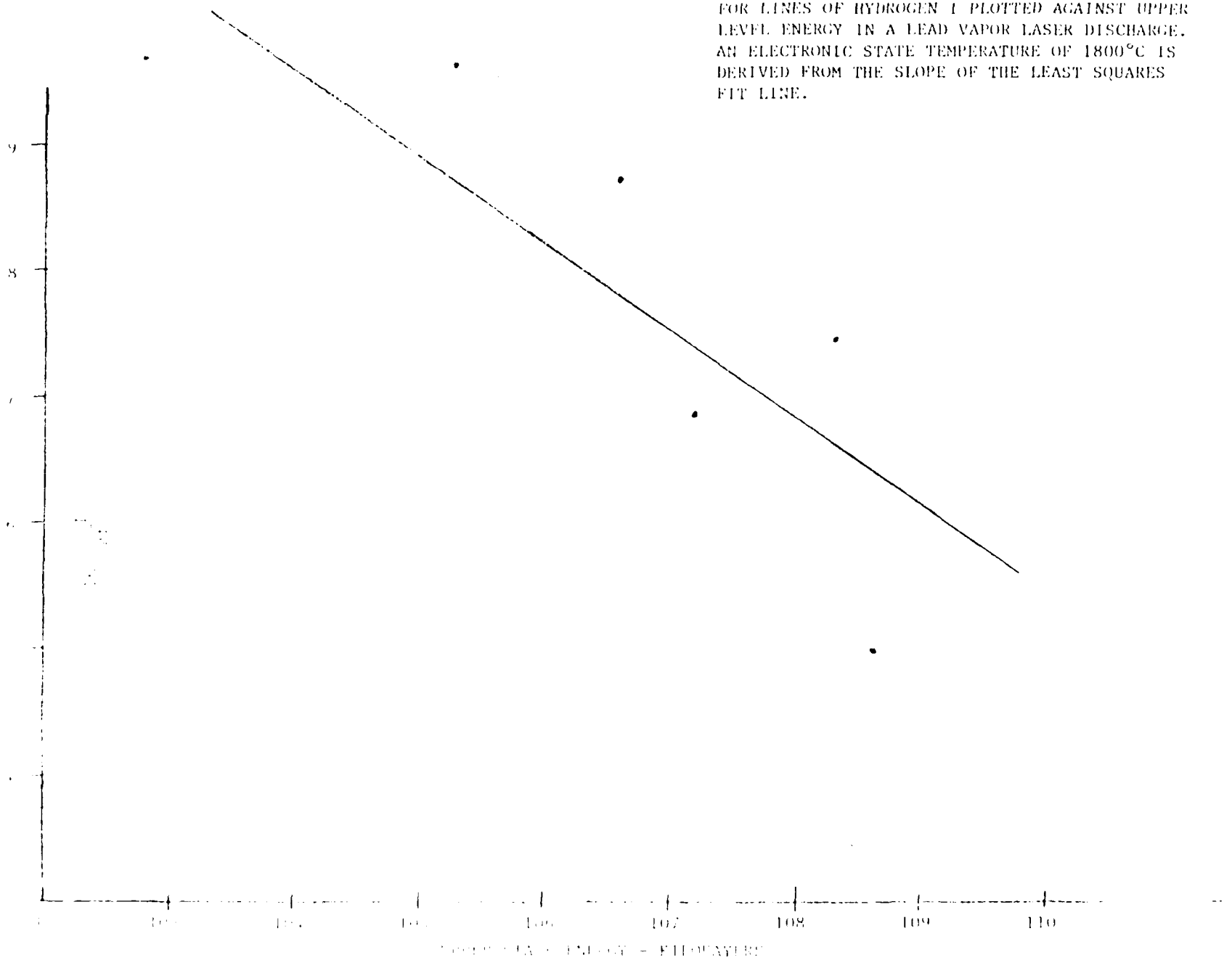

FIGURE 20. LOG RATIO OF LINE INTENSITY x λ^3 TO gf - VALUE FOR LINES OF LEAD VAPOR I PLOTTED AGAINST UPPER LEVEL ENERGY IN A LEAD VAPOR LASER DISCHARGE. AN ELECTRONIC STATE TEMPERATURE IS DERIVED FROM THE SLOPE OF THREE DIFFERENT LINES. AVERAGE TEMPERATURE IS 15,000°C.

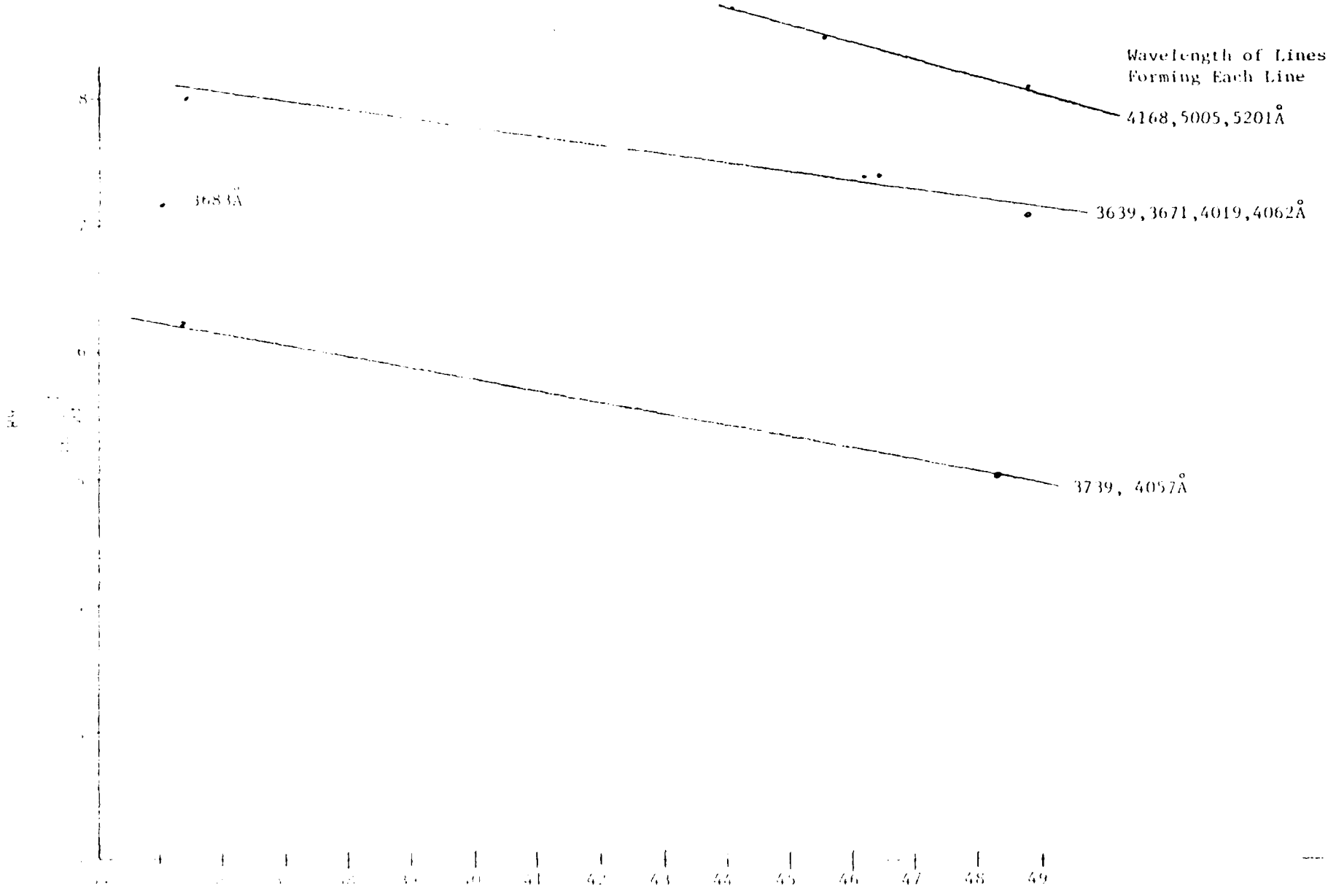

(temperature) can be seen on Figures 17 and 19 and three separate groups can be seen on Figure 20. Each line on Figure 20 is also associated with the spectral lines making it up and it can be seen that the points forming the upper two lines fall into two non-overlapping wavelength bands. Possibly operating conditions changed when the scan passed 4100 angstroms.

Even after accounting for the substantial scatter in the data the effective temperature associated with the three gases can be seen to be far exceeded by the temperature associated with the lead vapor.

This implies that different processes were involved in the excitation of the high lying (appproximately 13-24 eV) gas atom states and the low lying states (approximately 5 eV) of the lead vapor. Time resolved measurements made during an earlier IR&D program show helium emission to peak several microseconds after the discharge is extinguished, supporting an afterglow interpretation for the excitation of the gases. Direct electron excitation has been accepted for sometime as the mechanism for excitation of the metal.(15)

Consequently, in estimating contaminant partial pressures, a high temperature (15,000°C) was assumed only for easily excited species (e.g., lead, sodium, calcium, etc.)

That temperature was inserted in equation 1 and then the ratio of the intensity of a contaminant line to that of a lead line was made, e.g.,

$$\frac{I_{con}}{I_{Pb}} = \frac{N_{con}}{N_{Pb}} \frac{(gf)_{con}}{(gf)_{Pb}} \frac{\lambda^3_{Pb}}{\lambda^3_{con}} \frac{u_{Pb}}{u_{con}} \exp \frac{E_{Pb} - E_{con}}{kT} \qquad (3)$$

where subscripts con and Pb respectively apply to the contaminant and lead vapor. The only unknown in this expression is N_{con}, the contaminant partial pressure. The intensities are measured during our experiments and all other factors can be determined from the literature.[13,14]

This formulation could not be used for the gases excited by recombination in the afterglow. The cold Maxwellian electron energy distribution does not cause the excitation but is more likely heated by it. Consequently, while states lying within 0.2 eV of each other may be in equilibrium at the 1,500° temperature mentioned earlier, there is no coupling between different species of greatly differing level energies. Simultaneous solution of equation 1 for two different species will not lead to consistent results. The partial pressure of hydrogen and nitrogen must consequently be determined using a calibration of line intensity similar to that shown on Figure 16. Table 14 lists the calibration used and Table 15 the results when these procedures were used on a sealed-off lead vapor laser with a small leak.

Contaminant concentrations typical of a lead vapor laser with a flowing buffer gas after a long bakeout period are given in Table 16.

As was noted earlier, more effective clean-up can be achieved if higher temperatures are used to bakeout the laser tube. Consequently, a similar analysis was conducted for a copper vapor laser. Figure 21 shows a temperature determination using copper atom lines. It is interesting to note that the temperature of the copper vapor discharge was only about half of the lead vapor discharge.

Finally Table 17 shows the contaminant concentrations determined. The nitrogen gas, a dominant contaminant in early bakeout stages, is gone. Sodium

TABLE 14

CALIBRATION OF SPECTRAL LINE INTENSITY FOR PRESSURE

$$\text{Nitrogen Pressure} = \frac{\text{nitrogen } 5378\text{Å line inetnsity}}{\text{helium } 5047\text{Å line intensity}} \times .063 \text{ mm}$$

$$\text{Hydrogen Pressure} = \frac{\text{hydrogen } 4861\text{Å line intensity}}{\text{helium } 5047\text{Å line intensity}} \times .056 \text{ mm}$$

or

$$= \frac{\text{hydrogen } 4101\text{Å line intensity}}{\text{helium } 5047\text{Å line intensity}} \times .128 \text{ mm}$$

TABLE 15

PARTIAL PRESSURE OF CONTAMINANTS
IN A SEALED OFF LEAD VAPOR LASER

SPECIES	PARTIAL PRESSURE
Helium	21 mm
Hydrogen	.8 mm
Nitrogen	.7 mm
Sodium	.06 mm
Lead	.05 mm
Calcium	.002 mm

Input: 5 kV 328 ma
Tube Temperature: 795°C
Time Sealed: 17 hours
Seal Condition: Leak

TABLE 16

PARTIAL PRESSURE OF CONTAMINANTS
AFTER LONG RUN TIME IN A LEAD VAPOR LASER: TYPICAL VALUES

SPECIES	PARTIAL PRESSURE
Sodium	3×10^{-3} mm
Calcium	4×10^{-3} mm
Hydrogen	5×10^{-3} mm
Nitrogen	$\sim 10^{-4}$ mm

FIGURE 21. LOG RATIO OF LINE INTENSITY x λ^3 TO gf - VALUE FOR LINES OF COPPER VAPOR I PLOTTED AGAINST UPPER LEVEL ENERGY IN A COPPER VAPOR LASER DISCHARGE. A TEMPERATURE OF 7,472°K IS DERIVED FROM THE SLOPE

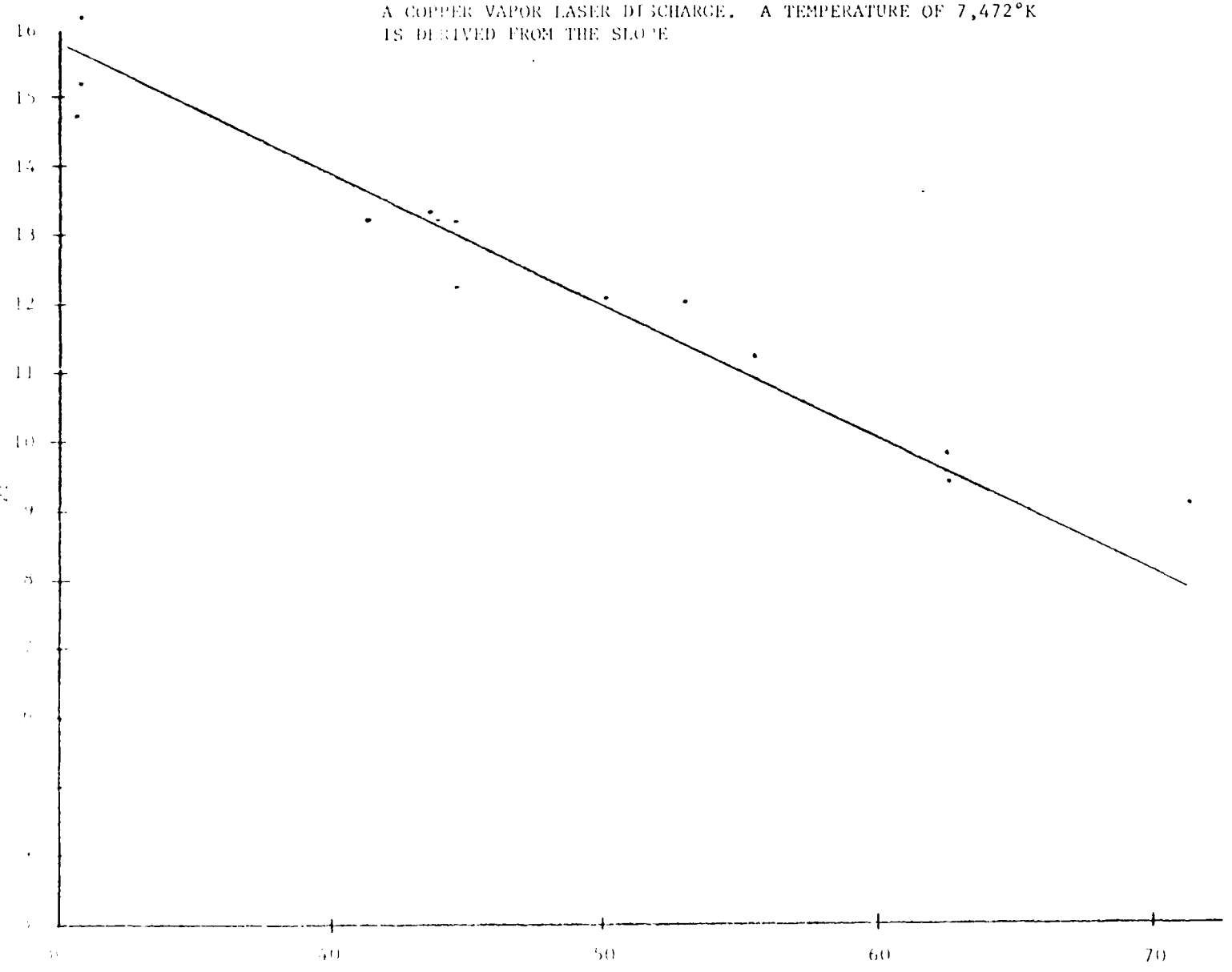

TABLE 17

PARTIAL PRESSURE OF CONTAMINANTS
IN A COPPER VAPOR LASER

SPECIES	PARTIAL PRESSURE
Helium	10 mm
Hydrogen*	.2 mm
Copper	2.5×10^{-3} mm
Calcium	2.5×10^{-5}
Magnesium	7.8×10^{-6}
Iron	7.7×10^{-6}
Sodium	1.6×10^{-6}
Chromium	1.06×10^{-6}

Power Input: 1890W
Tube Temperature: 1300°C
Output Power: 1W

*Purposely introduced with buffer to aid in wick element.

pressure has fallen so that calcium becomes most significant. Presumably the sodium source has been depleted while that of calcium, and other lower vapor pressure species, continues to evolve vapor.

When the laser tube has been oven baked at 1800°C for an extensive period (see Section VIII) even lower contaminant concentrations can ultimately be expected. Sodium line intensities over an order of magnitude below those obtained with discharge heating imply sodium partial pressure in the 10^{-8} mm range.

XII. CONCLUSIONS

It has been shown that the alumina ceramic discharge tubes are the principal long term source of contaminants. In early stages of heating nitrogen and hydrogen dominate but eventually metals such as sodium, calcium, etc. become more important. Bakeout temperatures as high as 1800°C are effective in removing these contaminants. Furnace heating is particularly attractive because of economy (when contrasted to discharge heating) and the extreme temperatures available. Contaminant partial pressures in the 10^{-6} mm range have been determined and inferred down to the 10^{-8} mm range. The problem of large variability (>50%) in the contaminants present in the vendor received tubes can only be solved by baking to some uniform level of cleanliness.

During the course of this work two significant analytical determinations were made. First, a simple model has been proven relating the time a wick of a given aspect ratio will contain metal. Lead vapor [illegible] maintained for over 200 [illegible] temperature has been used, pinhole [illegible] and 15,000°C in a lead vapor laser.

A new form of sealed laser with all seals at low temperature was used in some of this work. This development represents a significant advanced in its own right.

The detailed role that contaminants play in changing characteristics of the discharge and laser operation was not addressed. The distribution of power deposited within the discharge and the efficiency of laser excitation are profoundly affected. At times output power and laser efficiency are improved by the addition of a small quantity of another species with the buffer gas.

Continuation of the work described in this report could thus have practical as well as scientific benefit.

REFERENCES

1. R.S. Anderson, T.W. Karras, B.G. Bricks, and L.W. Springer, "Discharge Heated Copper Vapor Laser MOPA Operation," AFAL-TR-76-93 (1976).

2. R.S. Anderson, R.J. Homsey, and T.W. Karras, "Copper Vapor Laser Optimization," AFAL-TR-77-169.

3. I. Smilanski, G. Erez, A. Kerman, and L.A. Levin, "High Power, High Pressure, Discharge Heated Lead Vapor Laser," Optics Comm 30, 70 (1979).

4. B.G. Bricks, "Development of the Discharge-Heated Lead Vapor Laser," AFAL-TR-78-103 (1978).

5. R.J. Homsey and B.G. Bricks, Final Report to Contract F12-7F-02654/#3, "Pod Configuration of the Lead Vapor Laser Head Assembly for the Aireye Active Gated T.V. System," to be published.

6. "Instruction and Service Manual Discharge-Heated Copper Vapor Laser Model 6-15," General Electric Space Division (July 1979).

7. V.H. Burmakin, A.N. Evtyunin, M.A. Lesnoi, and V.I. Bylkin, "Long Life Sealed Copper Vapor Laser," Sov. J. Quant. Elec. 8, 574 (1978).

8. R.T. Hodgson, "Vapor Discharge Cell," United States Patent 3,654,567.

9. R.S. Anderson and T.W. Karras, "Copper Vapor Laser Lifetime Extension," Final Report to Lawrence Livermore National Laboratory Contract P.O. 5949703 (1977).

10. R.B. Keller, et al., "Copper Vapor Generator," AFWL-TR-73-223 (1974).

11. P.O. F12-7F-02654/#3.

12. Private Conversation, Richard Fanny, Coors Porcelain Company, Data Sheet supplied by McDaniel Ceramics Company.

13. C.H. Corliss and W.R. Bozman, "Experimental Transition Probabilities for Spectral Lines of Seventy Elements," National Bureau of Standards Monograph 53 (1962).

14. C.E. Moore, "Atomic Energy Levels," Circular of the National Bureau of Standards, 467 (1949).

15. D.A. Leonard, "Theoretical Description of the 5106 Angstrom Pulsed Copper Vapor Laser," IEEE J.O.E. QE-3, 38D (1967).

APPENDIX 1

SEALED OFF LEAD VAPOR LASER

GENERAL ELECTRIC
SPACE DIVISION
PHILADELPHIA

PROGRAM INFORMATION REQUEST / RELEASE

*CLASS. LTR.	OPERATION	PROGRAM	SEQUENCE NO.	REV. LT
PIR NO. U	— 1254 —		— 331	

*USE "C" FOR CLASSIFIED AND "U" FOR UNCLASSIFIED

FROM	TO
T.W. Karras	

DATE SENT	DATE INFO. REQUIRED	PROJECT AND REQ. NO.	REFERENCE DIR NO.
10/1/79			

SUBJECT

Sealed Off Lead Vapor Laser

INFORMATION REQUESTED/RELEASED

Abstract

A DHPbVL (lead vapor laser) has been operated in a sealed off mode without use of a vacuum pump for 78 hours. The cold window design involved no internal or high temperature seals and so is expected to be the prototype for very long term operation.

Previous pulsed metal vapor laser designs in this country have either involved a flowing gas[1], required a vacuum pump[2], or a high temperature vacuum seal[3,4]. The latter category has used a quartz tube with hot windows and appropriate high temperature feedthroughs for the electrodes[3] or a ceramic tube with high temperature ceramic to metal joints at its ends and a wicking system to confine the metal vapor[4]. While the continuous flow and vacuum pump are obviously undesirable the high temperature joints of the sealed alternative involves expensive and uncertain technologies.

An alternative approach is discussed here that involves only low temperature joints and cold windows. Consequently, seal lifetimes as long as those obtained with argon ion or even helium neon lasers might be achievable.

The basic approach uses a design similar to the discharge heated approach reported in the literature previously[2]. Figure 1 shows the elements of the design. The ceramic discharge tube contains an inert gas and two tubular wicks designed to supply and contain the metal vapor within the hot zone between them. A pair of tubular electrodes slip fit into the ends of the ceramic tube and also fit into holes in metal electrode flanges. The joints are not leak tight and so the inert gas also fills the annular space surrounding the ceramic tube. In addition, a high temperature thermal and electrical insulator fills that annular space but extends over the wicks only as far as necessary to maintain the proper temperature gradient along them. The annular insulator is so designed that for the desired discharge power deposited in the central tube the internal temperature will be sufficient to provide the desired metal vapor pressure. The outer surface of the annular insulator is in contact with a low temperature [illegible] which cools the vacuum wall with the environment. The annular insulator and the outer shell are sufficient electrical insulators so that in operation the voltage between the two electrode tubes will be constrained within the central discharge tube. It is this double function of the annular insulator that is the key.

C.E. Anderson D.M. Smith
R.S. Anderson L.W. Springer
B.G. Bricks
T.E. Burczacki
B.P. Fox
R.J. Hemsey
A.E. Kraft

PAGE NO. [illegible]

FORM 1020 B REV. 10-70

The only insulator to metal seals are those in the outer vacuum shell. Since these joints are in a low temperature region and see only minor temperature variation they should be both reliable and consistent with long life. This can be contrasted with high temperature seal designs which must inevitably place greater stress on this element.

The principal question in the test of such a design is the effectiveness of the electrically insulating section. The material of which it is made must be of sufficient diameter to thermally insulate the discharge tube and of sufficient length to prevent electrical breakdown.

Experiments have been conducted with a zirconia insulator 2½" in OD and about 13" long surrounding a 1" discharge tube filled with lead. The vacuum shell was made from copper gasketed VARIAN components and Ceradyne vacuum breaks. The windows were attached through glass to kovar tubular seals. All metal bellows valves were used to evacuate and fill the device.

The apparatus was first outgassed by running in a flowing mode without lead in the tube. The tube was then sealed off and run for a time to determine the new input power requirements; since with gas in the annular region more power would now be needed to reach operating temperatures.

Finally, the laser was opened, lead added to the wicks, and degassing of the lead took place by running the laser in a flowing mode. The sealed off laser run followed.

The zirconia insulator survived 184 hours of running and bakeout time. The laser run involved 108 hours continuously sealed off and 78 hours of sealed off lasing. The test was halted by either a leak in a vacuum break or breakage of the discharge tube near an electrode, failures believed to be irrelevant to the component under test.

The characteristics of the run are listed in Table I.

TABLE I

Fill Buffer Gas	Helium 22 mm Hot 16.5 mm Cold
Power Supply Voltage Current	 4.8 KV 380-400 ma
Discharge Tube Temperature	900°C (880°C - 920°C)
Average Output Power	.2 - .3 W
Sealed Off Lasing Time	78 Hours
Sealed Off Time	108 Hours

The laser operating conditions were by no means optimum. A slightly larger diameter zirconia insulator would reduce the input power requirements. The vacuum breaks making up the external insulator where old and patched RTV. Finally, the wicks were of an unreliable short lifetime design and consequently unsuitable for long term testing.

It is interesting to note that the laser output power gradually rose during the course of this run. This may be due to non-congruent discharge pumping of contaminants.

Before and during the sealed off tests a series of spectroscopic studies of the contaminants present in the discharge were undertaken. They will be reported on elsewhere.

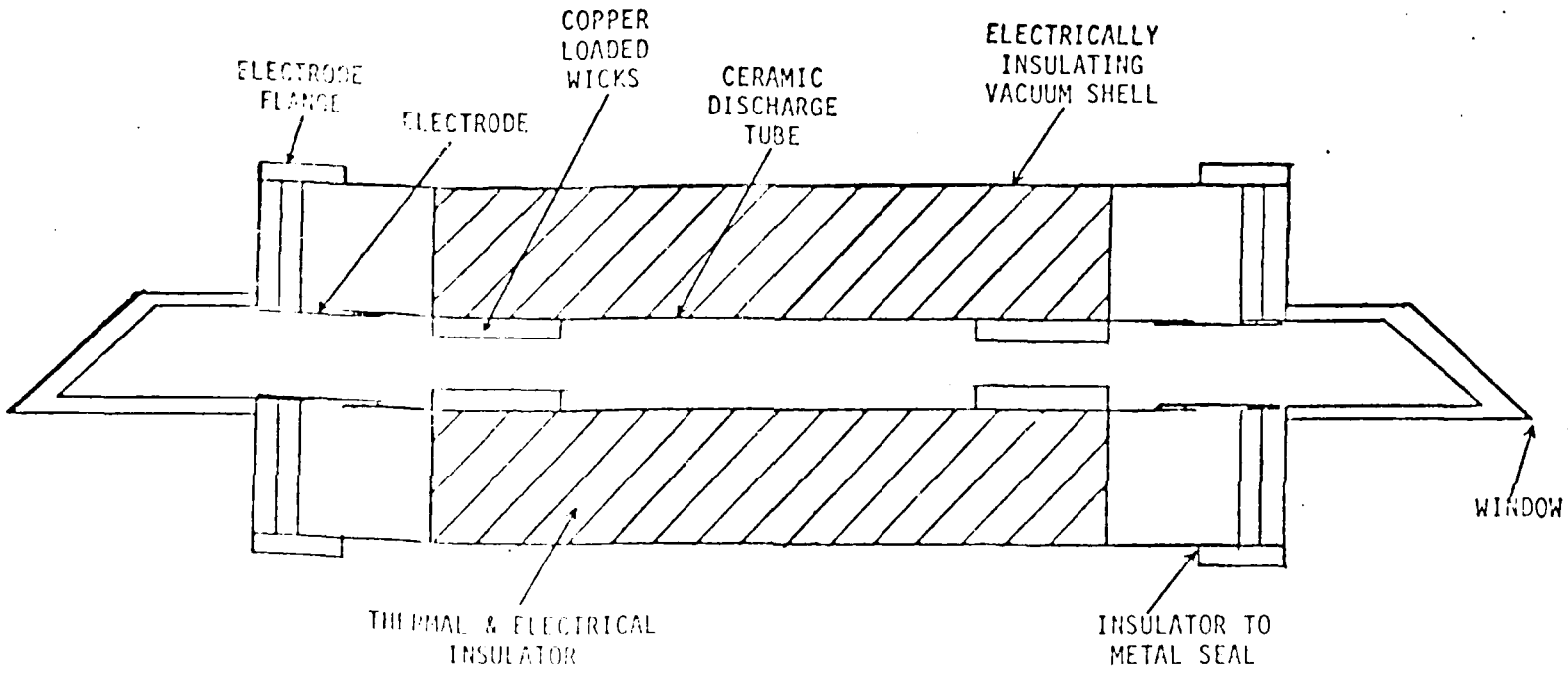

Figure 1. Schematic of Sealed-off Design

REFERENCES

1. B.G. Bricks, T.W. Karras, R.S. Anderson, and C.E. Anderson, "Results of a Parametric Study of a Flowing Copper Vapor Laser", Bull. Am. Phys. Soc. 22 190 (1977).

2. R.S. Anderson, L.W. Springer, B.G. Bricks, and T.W. Karras, "A Discharge Heated Copper Vapor Laser", IEEE J. Quant. Elec. QE-11 173 (1975).

3. D.W. Feldman, C.S. Liu, J.L. Pack, and L.A. Weaver, "Long-lived Sealed Off Lead Vapor Lasers", "Presented at the Conference on Laser and Electro-optical Systems", San Diego, Calif.

4. B.G. Bricks, M.J. Linevsky, R.J. Homsey, and T.W. Karras, "Discharge Heated Metal Vapor Laser Studies II", G.E. TIS 78SD017 (1978).

APPENDIX 2

WINDOW COATING STUDY

GENERAL ELECTRIC
SPACE DIVISION
PHILADELPHIA

PROGRAM INFORMATION REQUEST / RELEASE

	*CLASS. LTR.	OPERATION	PROGRAM	SEQUENCE NO.	REV. LTR.
PIR NO.	U	— 1254	—	— 302	

*USE "C" FOR CLASSIFIED AND "U" FOR UNCLASSIFIED

FROM	TO
T. W. Karras	C. E. Anderson

DATE SENT	DATE INFO. REQUIRED	PROJECT AND REQ. NO.	REFERENCE DIR. NO.
7/16/79			

SUBJECT

WINDOW COATING STUDY

INFORMATION REQUESTED/RELEASED

It has been discovered that after the first few hours of operation, which might most properly be called bakeout or clean out, copper vapor laser window coating is due to discharge sputtering of the metal near the window. Electron beam probe analyses have found iron, chromium and other constituents of stainless steel in the window coating. In addition, their proportions have roughly corresponded to those found in the metal making up the window assembly.

In order to prevent this coating a glass tube has been placed inside of the window assembly of a standard Model 6-15 CVL and butted against the window. The tube was 1" ID, 1-3/16" OD, 2-5/8" long, and cut at Brewsters angle so there was as little space as possible between the glass tube and the window (Figure 1). Consequently the discharge could not attach anywhere near the window.

As long as the tube lay against the window in this way no further window coating has been observed. Figure 1 shows the photograph of a glass discharge barrier tube run for 30-40 hours.

Of course the flat end of the glass tube was adjacent to the discharge and so sputtering coating was found both inside and outside of the tube near that end. Figure 2 gives the optical transmission of that coating as a function of distance from the flat end of the tube. This should be a measure of the coating thickness and the distance sputtered material can travel.

Two distinct regions can be identified in both Figures 1 and 2. A thick opaque coating on the outside of the tube ends from 7-9 mm from the tube end. A thin but more adherent coating ends about 14 mm away from the discharge. Some slight coating exists even beyond this and may represent a third region.

cc: G. Bricks
R. Homsey

PAGE NO.

FORM 1020B REV. (9-75)

I suspect that different mechanisms are involved in each of these regions but no effort has been expended to understand them. For the purpose of this study all we can say is that a glass tube acts as a satisfactory discharge barrier to prevent sputter coating of the window. The flat end of the tube must extend at least 2-3 cm away from the window ($L/D \sim 1$). Greater than 4.6 cm might be necessary for run times of many hundreds of hours or longer.

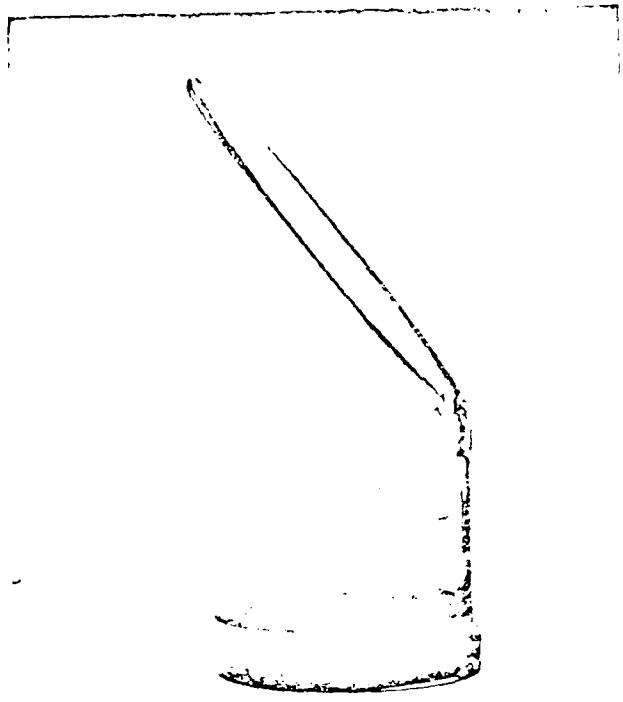

Figure 1. Photograph of Glass Discharge Barrier Tube. Sputter coating can be seen near flat end.

AD-A100 906 GENERAL ELECTRIC CO PHILADELPHIA PA SPACE DIV F/G 20/5
METAL VAPOR LASER CONTAMINANT STUDY.(U)
MAY 80 T W KARRAS, B G BRICKS F49620-79-C-0177
UNCLASSIFIED AFOSR-TR-81-0520 NL

2 OF 2
AD A
100906

END
DATE FILMED
7-81
DTIC

Figure 2. Transmission of Sputtered Coating on Glass Discharge Barrier

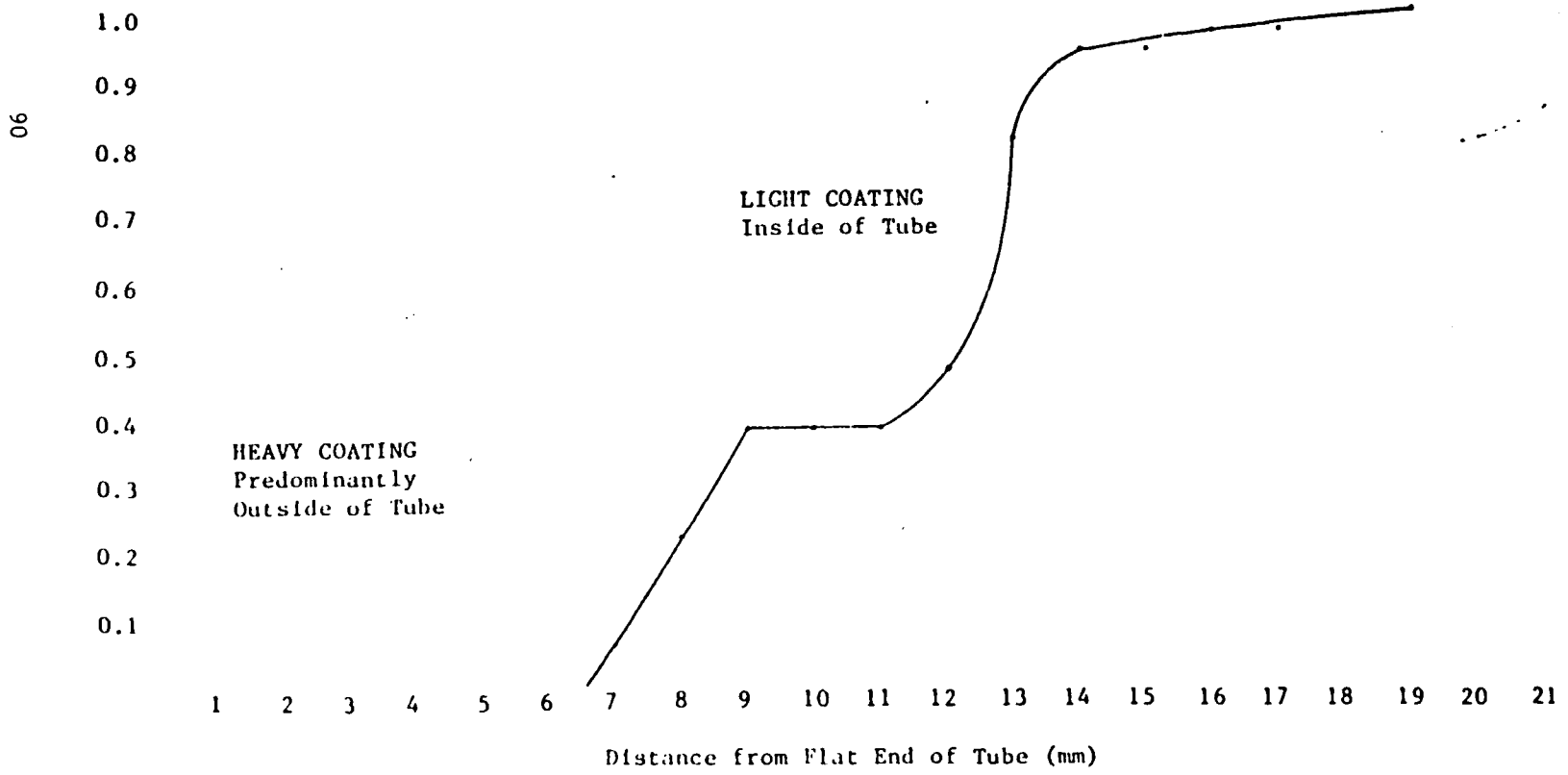

APPENDIX 3

DESIGN OF WICKS FOR METAL VAPOR LASERS

GENERAL ELECTRIC
SPACE DIVISION
PHILADELPHIA

PROGRAM INFORMATION REQUEST / RELEASE

PIR NO.	*CLASS. LTR.	OPERATION	PROGRAM	SEQUENCE NO.	REV. LTR.
	U	— 1254 —		— 349	

*USE "C" FOR CLASSIFIED AND "U" FOR UNCLASSIFIED

FROM	TO
T.W. Karras & B.G. Bricks	Distribution

DATE SENT	DATE INFO. REQUIRED	PROJECT AND REQ. NO.	REFERENCE DIR. NO.
2/19/80			

SUBJECT

Design of Wicks for Metal Vapor Lasers

INFORMATION REQUESTED/RELEASED

Metal vapor lasers are limited in the amount of time they can operate without attention by the time it takes for metal to diffuse out of the hot zone. Metal placed in the center of a low buffer pressure copper vapor laser tube will thus be lost in a few hours.

In order to extend this time, techniques for recirculating metal have been used. The most common and most effective uses a wick structure that, once the metal vapor diffuses into cool regions and condenses upon the wick surface, will draw the metal fluid back into the hot zone[1-4]. There it will vaporize again making it available for lasing and repeat of the diffusion cycle.

The most commonly used structure involves a cylindrical element placed on the inside walls at either end of a discharge tube. The diameter of the wick is thus fixed by the inner diameter of the discharge tube. The thickness of the wick wall should be minimized to prevent obscuration of the active volume but will in general be fixed by the type of structure used. The only dimension left free is then the length of the wick.

In the simple steady state diffusion of metal vapor through a buffer gas, with mean free path very small and with the diffusion coefficient assumed constant, the metal vapor concentration obeys Laplace's equation. In cylindrical coordinates, assuming the vapor concentration, ρ, goes to zero at the walls (unity accommodation coefficient) and also assuming radial symmetry, at a finite distance into the tube the solution depends inverse exponentially upon the distance into the wick z, as shown below.

C.E. Anderson
T.E. Buczacki
R.J. Homsey
D.M. Smith
L.W. Springer

PAGE NO 1 OF 5

RETENTION REQUIREMENTS

COPIES FOR	MASTERS FOR
1 MO.	3 MOS.
3 MOS.	6 MOS.
6 MOS.	12 MOS.
MOS.	MOS.
	DONOTDES'R

$$\rho = \rho_0 e^{-kz} J_0(kr) \qquad (1)$$

Here $k = 2.405/a$, 2.405 is the first zero of the Bessel function, J_0, and "a" is the cylindrical wick internal radius. For vapor diffusion velocity independent of distance z the flow rate F lost out of the cool end of the wick can be expressed in terms of the length to diameter ratio of that wick, $\ell/d = x$, as

$$F = F_0 e^{+k'x} \qquad (2)$$

where F_0 is the loss rate for $x = 0$ and $k' = 4.8$. The time a metal vapor laser can operate before its store of metal, S, has been lost is then given by

$$T = \frac{S}{F} = \frac{S}{F_0} e^{-k'x}. \qquad (3)$$

Under realistic experimental conditions the accommodation coefficient for metal atoms to stick to the wick surface will be less than unity. Furthermore there will be a temperature and axial distance dependence for the diffusion constant, vapor velocity, and wick recirculation (wetting) properties. These factors will all tend to increase the flow rate (vapor loss rate) by decreasing k' in Equations (2) and (3).

A series of experiments have been performed that support this model. Discharge heated copper[5] and lead vapor lasers[6] were used with a variety of wick length and diameters. In all cases the metal vapor pressure within the laser was about 0.1 torr. Figure 1 plots the time it took for the laser power to fall by 20%, presumably due to depletion of metal in the wicks, as a function of the length to diameter ratio of those wicks. Two sets of data are shown, one with wicks carefully discharge cleaned before loading and one without special preparation.

The expected exponential dependence is followed very closely. For both sets of data the value of k' was .96 - .97, considerably below the ideal indicated earlier.

The effect of wick cleaning appears as a shift or raising of the curve so that $\Delta x = 1.4$ or $\Delta \frac{S}{F_0}\Big|^{\ell=0}$ = (.88 clean - .22 as is) = .66 hrs. This cannot be attributed to a change in F_0 since that has purely geometrical dependence.

However, incomplete wetting of the wick due to incomplete cleaning can reduce the effective length, x, and the available metal supply, S. It is expected that this effect takes place at the output end of the wick. This cool end of the wick is most susceptible to such an effect because wetting forces are weakest at low temperatures.

In summary, a model has been successfully demonstrated that relates the metal vapor containment time to be expected with wicks of given dimensions. This containment time has also been quantitatively related to two different procedures for wick cleaning. Since the same curves have been found to be applicable for two different metals and several different length and wick diameters the model is expected to be generally applicable.

Figure 1

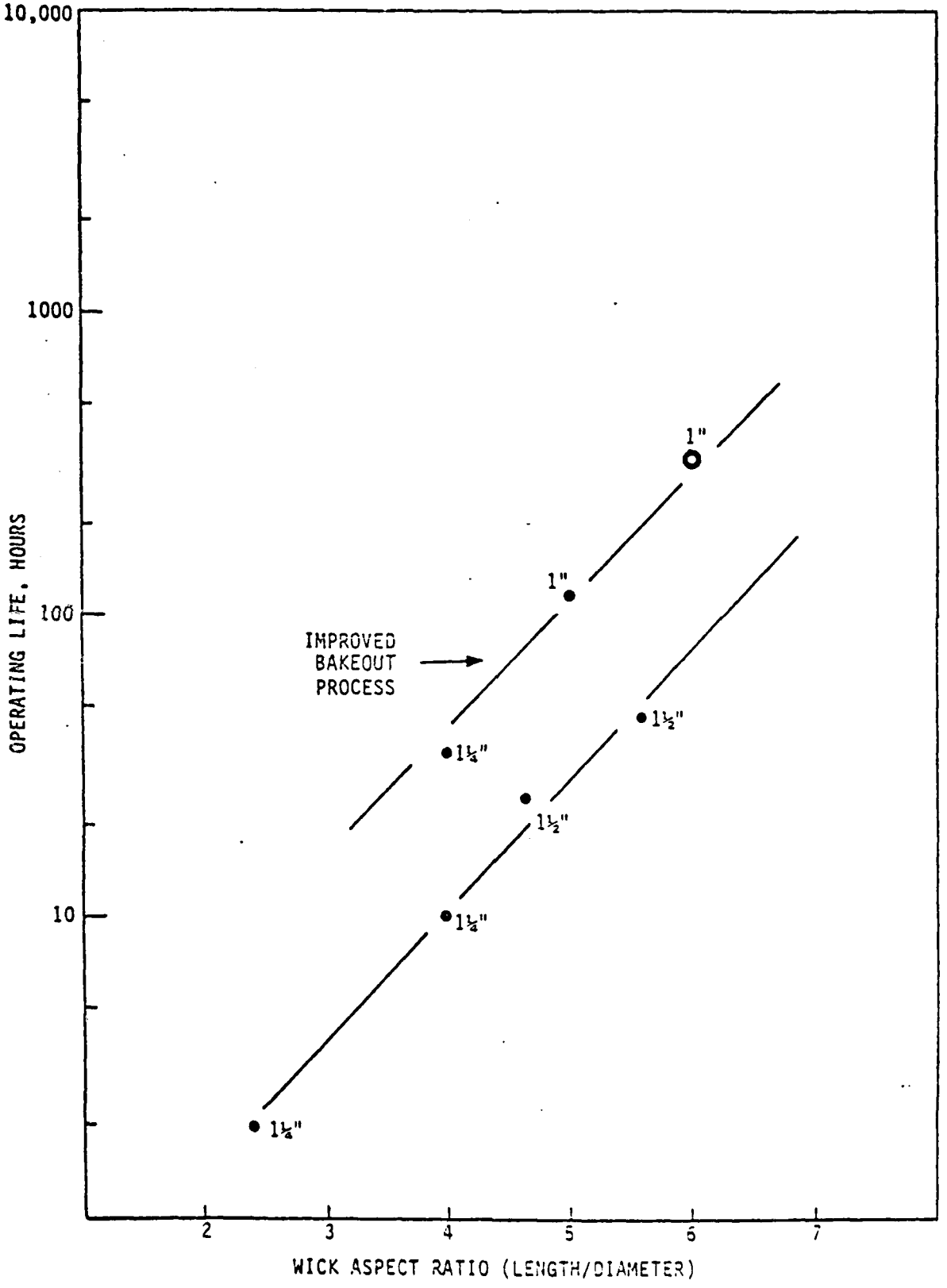
10,000
1000
100
10
OPERATING LIFE, HOURS
IMPROVED
BAKEOUT
PROCESS
1"
1"
1½"
1½"
1½"
1½"
1½"
2
3
4
5
6
7
WICK ASPECT RATIO (LENGTH/DIAMETER)

REFERENCES

1. R.T. Hodgson, "Vapor Discharge Cell", Patent 3,654,567 (1972).

2. P.H. Bokham et al, Pribory; Tekhnika Eksperimenta 1 160 (1974).

3. R.J.L. Chimenti, "Heat Pipe Copper Vapor Laser", Final Report to Contract N00014-73-C-0317, NT 15 AD768-364/26A (1973).

4. P.H. Cahuzac and X. Drago, Optics Communications 18 600 (1976).

5. R.S. Anderson, L.W. Springer, B.G. Bricks and T.W. Karras, IEEE J. Quant. Elect. QE-11 172 (1975).

6. B.G. Bricks and T.W. Karras, Presented at Lasers '79, Orlando, Florida, December 1979.

APPENDIX 4

RELATIONSHIP BETWEEN METAL VAPOR DENSITY AND LASER OUTPUT POWER

In going from 890°C to 915°C in the sealed-off lead vapor laser of Section IX, the vapor pressure of lead rises by 1 [illegible] torr to .37 torr) and the vapor density by 1.45. The observed rise in power, .23 W to .31 W, is a factor of 1.35. This is close enough to support a linear relationship between lead vapor density and output power in this range of the parameters.

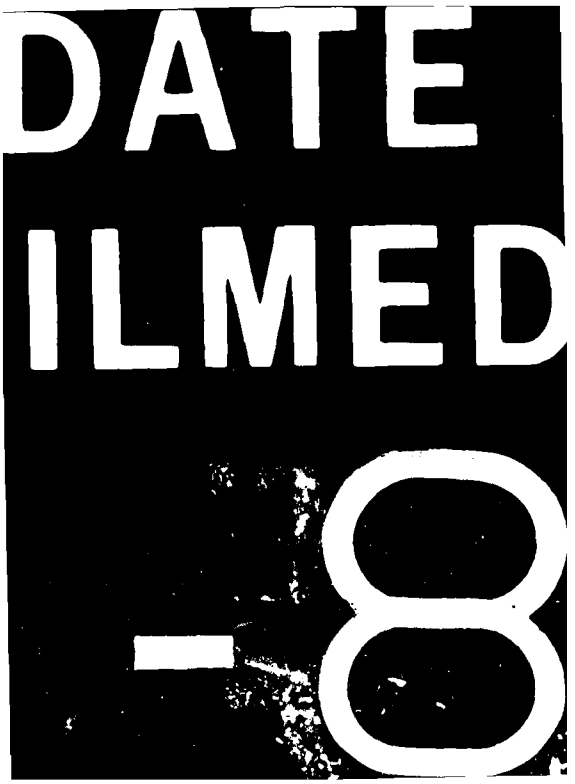
DATE
ILMED
-8